

# Reproductive Toxicology

## BPA disrupts meiosis I in oogonia by acting on pathways including cell cycle regulation, meiosis initiation and spindle assembly.

--Manuscript Draft--

<b>Manuscript Number:</b>	RTX-D-22-00004R2		
<b>Article Type:</b>	Full Length Article		
<b>Keywords:</b>	fetal ovary; organ culture; meiosis; oogonia; BPA; sheep		
<b>Corresponding Author:</b>	Béatrice Mandon-Pépin, Ph.D. INRAE Centre Île-de-France Jouy-en-Josas Antony: Institut National de Recherche pour l'Agriculture l'Alimentation et l'Environnement Centre Ile-de-France Jouy-en-Josas Antony Jouy-en-Josas, Île-de-France FRANCE		
<b>First Author:</b>	Benoit Loup, Ph.D.		
<b>Order of Authors:</b>	Benoit Loup, Ph.D. Elodie Poumerol Luc Jouneau Paul A Fowler Corinne Cotinot Béatrice Mandon-Pépin, Ph.D.		
<b>Manuscript Region of Origin:</b>	Europe		
<b>Abstract:</b>	<p>The negative in utero effects of BPA on female reproduction are of concern since the ovarian reserve of primordial follicles is constituted during the fetal period. This time-window is difficult to access, particularly in humans. Animal models and explant culture systems are, therefore, vital tools for investigating EDC impacts on PGCs. Here, we investigated the effects of BPA on prophase I meiosis in the fetal sheep ovary. We established an in vitro model of early gametogenesis through retinoic acid-induced differentiation of sheep PGCs that progressed through meiosis. Using this system, we demonstrated that BPA (<math>3 \times 10^{-7}M</math>, <math>3 \times 10^{-5}M</math>) exposure for 20 days disrupted meiotic initiation and completion in sheep oogonia and induced transcriptomic modifications of exposed explants. After exposure to the lowest concentrations of BPA (<math>3 \times 10^{-7}M</math>), only 2 probes were significantly up-regulated corresponding to NR2F1 and TMEM167A transcripts. In contrast, after exposure to <math>3 \times 10^{-5}M</math> BPA, 446 probes were deregulated, 225 were down- and 221 were up-regulated following microarray analysis. Gene Ontology (GO) annotations of differentially expressed genes revealed that pathways mainly affected were involved in cell-cycle phase transition, meiosis and spindle assembly. Differences in key gene expression within each pathway were validated by qRT-PCR.</p> <p>This study provides a novel model for direct examination of the molecular pathways of environmental toxicants on early oogenesis and novel insights into the mechanisms by which BPA affects meiosis I. BPA exposure could thereby disrupt ovarian reserve formation by inhibiting meiotic progression of oocytes I and consequently by increasing atresia of primordial follicles containing defective oocytes.</p>		
<b>Suggested Reviewers:</b>	Severine Mazaud-Guittot, Dr Researcher, Rennes 1 University: Universite de Rennes 1 severine.mazaud@univ-rennes1.fr Works on endocrine disruptors and fetal gonads	Richard Lea University of Nottingham School of Veterinary Medicine and Science richard.lea@nottingham.ac.uk Works on endocrine disruptors on ruminants	Virginie Rouiller-Fabre, Professor Institut de biologie François Jacob: Commissariat a l'energie atomique et aux energies

	<p>alternatives Institut de biologie Francois Jacob virginie.rouiller-fabre@cea.fr Works on endocrine disruptors and mouse gonads</p>
	<p>Pauliina Damdimopoulou, Dr PI, KI: Karolinska Institutet pauliina.damdimopoulou@ki.se Works on effects of chemicals on reproductive health in women</p>
	<p>Catherine Viguié, Dr, DMV Research Director, INRAE Occitanie-Toulouse: Institut National de Recherche pour l'Agriculture l'Alimentation et l'Environnement Centre Occitanie-Toulouse catherine.viguie@inrae.fr Works on understanding the toxicokinetic mechanisms leading to fetal exposure to endocrine disruptors.</p>
	<p>Gabriel Livera, Dr Pr, CEA Jacob: Commissariat a l'energie atomique et aux energies alternatives Institut de biologie Francois Jacob gabriel.livera@cea.fr Works on the different stages of fetal meiosis - effects of endocrine disruptors</p>
<p><b>Response to Reviewers:</b></p>	

## Highlights

- Development of a meiosis targeting culture model of the fetal ovary in sheep.
- BPA reduced the expression of meiotic marker genes in exposed explants.
- BPA altered expression of genes involved in cell cycle transition, meiosis, and spindle formation.
- Long-term effects could result in a reduction of the ovarian reserve and an increased frequency of aneuploidy.

**ABSTRACT**

The negative *in utero* effects of BPA on female reproduction are of concern since the ovarian reserve of primordial follicles is constituted during the fetal period. This time-window is difficult to access, particularly in humans. Animal models and explant culture systems are, therefore, vital tools for investigating EDC impacts on PGCs. Here, we investigated the effects of BPA on prophase I meiosis in the fetal sheep ovary. We established an *in vitro* model of early gametogenesis through retinoic acid-induced differentiation of sheep PGCs that progressed through meiosis. Using this system, we demonstrated that BPA ( $3 \times 10^{-7} \text{M}$ ,  $3 \times 10^{-5} \text{M}$ ) exposure for 20 days disrupted meiotic initiation and completion in sheep oogonia and induced transcriptomic modifications of exposed explants. After exposure to the lowest concentrations of BPA ( $3 \times 10^{-7} \text{M}$ ), only 2 probes were significantly up-regulated corresponding to NR2F1 and TMEM167A transcripts. In contrast, after exposure to  $3 \times 10^{-5} \text{M}$  BPA, 446 probes were deregulated, 225 were down- and 221 were up-regulated following microarray analysis. Gene Ontology (GO) annotations of differentially expressed genes revealed that pathways mainly affected were involved in cell-cycle phase transition, meiosis and spindle assembly. Differences in key gene expression within each pathway were validated by qRT-PCR.

This study provides a novel model for direct examination of the molecular pathways of environmental toxicants on early oogenesis and novel insights into the mechanisms by which BPA affects meiosis I. BPA exposure could thereby disrupt ovarian reserve formation by inhibiting meiotic progression of oocytes I and consequently by increasing atresia of primordial follicles containing defective oocytes.

1 **BPA disrupts meiosis I in oogonia by acting on pathways including cell cycle**  
2 **regulation, meiosis initiation and spindle assembly**

3

4 **Benoit Loup<sup>a</sup>, Elodie Pומרol<sup>a</sup>, Luc Jouneau<sup>a</sup>, Paul A Fowler<sup>b</sup>, Corinne**  
5 **Cotinot<sup>a</sup>, Béatrice Mandon-Pépin<sup>a\*</sup>**

6

7 <sup>a</sup> Université Paris-Saclay, UVSQ, ENVA, INRAE, BREED, 78350, Jouy-en-Josas,  
8 France; [loup\\_benoit@hotmail.com](mailto:loup_benoit@hotmail.com) (BL); [elodie.pומרol@inrae.fr](mailto:elodie.pומרol@inrae.fr) (EP);  
9 [luc.jouneau@inrae.fr](mailto:luc.jouneau@inrae.fr) (LJ); [p.a.fowler@abdn.ac.uk](mailto:p.a.fowler@abdn.ac.uk) (PAF); [corinne.cotinot@inrae.fr](mailto:corinne.cotinot@inrae.fr)  
10 (CC).

11

12 <sup>b</sup> Institute of Medical Sciences, School of Medicine, Medical Sciences & Nutrition,  
13 University of Aberdeen, Foresterhill, Aberdeen, AB25 2ZD, UK.

14

15

16 \* **Corresponding author:** [beatrice.mandon-pepin@inrae.fr](mailto:beatrice.mandon-pepin@inrae.fr) (BMP); phone: +0033-  
17 134652567

18 Full postal address: INRAE, UMR BREED, Batiment 230/231, Domaine du Vilvert,  
19 78350 Jouy en Josas, France

20

21

22 **ABSTRACT**

23 The negative *in utero* effects of bisphenol A (BPA) on female reproduction are of  
24 concern since the ovarian reserve of primordial follicles is constituted during the fetal  
25 period. This time-window is difficult to access, particularly in humans. Animal models  
26 and explant culture systems are, therefore, vital tools for investigating EDC impacts on  
27 primordial germ cells (PGCs). Here, we investigated the effects of BPA on prophase I  
28 meiosis in the fetal sheep ovary. We established an *in vitro* model of early  
29 gametogenesis through retinoic acid (RA)-induced differentiation of sheep PGCs that  
30 progressed through meiosis. Using this system, we demonstrated that BPA ( $3 \times 10^{-7}$  M  
31 &  $3 \times 10^{-5}$  M) exposure for 20 days disrupted meiotic initiation and completion in sheep  
32 oogonia and induced transcriptomic modifications of exposed explants. After exposure  
33 to the lowest concentrations of BPA ( $3 \times 10^{-7}$  M), only 2 probes were significantly up-  
34 regulated corresponding to NR2F1 and TMEM167A transcripts. In contrast, after  
35 exposure to  $3 \times 10^{-5}$  M BPA, 446 probes were deregulated, 225 were down- and 221  
36 were up-regulated following microarray analysis. Gene Ontology (GO) annotations of  
37 differentially expressed genes revealed that pathways mainly affected were involved  
38 in cell-cycle phase transition, meiosis and spindle assembly. Differences in key gene  
39 expression within each pathway were validated by qRT-PCR.

40 This study provides a novel model for direct examination of the molecular pathways of  
41 environmental toxicants on early female gametogenesis and novel insights into the  
42 mechanisms by which BPA affects meiosis I. BPA exposure could thereby disrupt  
43 ovarian reserve formation by inhibiting meiotic progression of oocytes I and  
44 consequently by increasing atresia of primordial follicles containing defective oocytes.

45

46 **Keywords:** fetal ovary, organ culture, meiosis, oogonia, BPA, sheep

47

48 **Abbreviations:**

49 RA, Retinoic acid; BPA, Bisphenol A; AM580, retinoic acid receptor agonist; STRA8,  
50 Stimulated by Retinoic acid gene 8; PGC, primordial germ cell; DPC, days post  
51 coitum; SAC, spindle assembly checkpoint; COC, cumulus–oocyte complex;

52

53 **Highlights**

54

- 55 • Development of a meiosis targeting culture model of the fetal ovary in sheep.
- 56 • BPA reduced the expression of meiotic marker genes in exposed explants.
- 57 • BPA altered expression of genes involved in cell cycle transition, meiosis, and  
58 spindle formation.
- 59 • Long term effects could result in a reduction of the ovarian reserve and an  
60 increased frequency of aneuploidy.

61

62

## 63 1. Introduction

64 Following initiation of the female cascade by the WNT4/RSP01/ $\beta$ -catenin pathway,  
65 granulosa cell fate is enforced by expression of FOXL2 in XX fetal gonads[1–5]. This  
66 somatic sex determination occurs from around 8 weeks of gestation in human ovaries  
67 [6], 34-36 days *post coitum* (*dpc*) in the sheep and goat, [7,8] and 12.5 *dpc* in mouse  
68 [9]. Following sex determination commitment, a species-dependent period of ovarian  
69 somatic and germ cell proliferation occurs [10], influenced by estrogens in non-rodent  
70 mammals [11]. Next, the primordial germ cells (PGC) switch from mitosis to meiosis.  
71 The onset of meiosis is, at least in part, triggered by retinoic acid [12,13], which  
72 stimulates the up-regulation of the pre-meiosis marker STRA8 and, subsequently, the  
73 meiotic signalling cascade that includes SYCP1, SPO11 and DMC1, [13–15]. In sheep,  
74 this occurs around 55 *dpc* [7,16]. Once germ cells are blocked in diplotene at the end  
75 of prophase I and enclosed in ovigerous nests, primordial follicle formation then  
76 commences, at around 75 *dpc* in sheep [17]. Like other female mammals, the sheep  
77 oocytes within the primordial follicles remain arrested in the first meiotic division until  
78 the re-activation of follicles in the postnatal ovary. These constitute the ovarian reserve  
79 that is established for the entire reproductive life of females.

80 There are notable differences regarding the differentiation processes of the  
81 mammalian fetal ovary [18]. While in sheep and cattle, similar to humans, meiosis and  
82 follicle development progresses from the inner to the outer regions of the cortex, in  
83 rodents these events progress in an anterior to posterior direction. This may signal  
84 species differences either in the site of retinoic acid production (mesonephros vs ovary)  
85 or in the timing and organization of mesonephric cell penetration of the cortex [18].  
86 Collectively, these studies indicate that, the production and/or delivery of factors and  
87 signalling mechanisms involved in the initiation of meiosis is the subject of species



88 differences between rodents and larger mammals [18]. In species with delayed  
89 meiosis, such as sheep and humans, there is an extended period between gonadal  
90 sexual differentiation and the onset of meiosis. An intense germ cell proliferation phase  
91 occurs during this period. In the developing sheep ovary, germ cell numbers increase  
92 from approximately 50,000 to 805,000 [19]. This proliferative period coincides with a  
93 peak in aromatase expression and oestrogen production. While the ovary does not  
94 produce steroids during early fetal life in mice [20], in many other mammalian species,  
95 such as ruminants and humans, the developing ovary is steroidogenically active [21–  
96 25]. Therefore, these species may be particularly sensitive to estrogen-mimetic  
97 compounds, unlike rodents.

98

99 Bisphenol A [BPA; 2, 2-bis (4-hydroxyphenyl) propane; CAS#80-05-7] is one of the  
100 most widely produced chemicals globally and is an endocrine disrupting compound  
101 (EDC) that can affect ovarian development as it can bind to estrogen receptors [26-  
102 27]. Adult mouse oocytes exposed to BPA exhibit improperly aligned chromosomes at  
103 the spindle equator during metaphase II and unbalanced chromosome sets while pups  
104 derived from exposed oocytes have higher abortion rates than controls [28–32].

105 However, the cellular and molecular processes are very different between fetal meiosis  
106 (initiation from oogonia in mitosis, homologous recombination then arrest in prophase I  
107 at the diplotene stage) and adult meiosis (activation of small groups of oocytes I  
108 regulated FSH and LH signaling, reductional meiosis which will give two cells of  
109 different sizes. Then after ovulation, the oocyte II engages in its second division of  
110 meiosis but will be blocked in metaphase II. The extrapolation of the effects observed  
111 on oocytes II of adult mice to human fetal oogonia is questionable. This is why we  
112 proposed a culture model of fetal gonads in a species presenting characteristics of

113 ovarian differentiation close to human to elucidate mechanisms involved in adverse  
114 impacts of EDCs on fetal ovary differentiation. Very few studies have been published  
115 in humans for ethical reasons and the scarcity of biological material. They show that  
116 human fetal BPA-exposed oocytes exhibit delayed meiotic progression, characterised  
117 by a fall in the percentage of oocytes reaching pachytene and a reduced oocyte viability  
118 in culture [33].

119

120 The sheep was selected as a relevant generic model for the extrapolation of BPA fetal  
121 kinetics to the human fetus because it is an acknowledged model for characterizing  
122 BPA disposition during the prenatal period [34]. Furthermore, BPA glucuronidation in  
123 humans and sheep is very similar [35,36].

124 We developed an *ex vivo* culture model on sheep fetal ovary that recapitulates the key  
125 stages of prophase I meiosis in oogonia. Using this ovarian explant culture, we  
126 investigated the effects of BPA on early female gametogenesis, identifying possible  
127 underlying mechanisms. Ranges of total BPA concentrations in human pregnancy are:  
128 maternal plasma 1.5–80 ng/mL [37,38], amniotic fluid 0.3-10 ng/mL [39–42], and cord  
129 blood 0.1-50 ng/mL [43–45].

130 It is noteworthy that the results obtained in near-term fetuses are not necessarily  
131 representative of BPA fetal exposure at earlier stages of pregnancy. As shown by  
132 Corbel et al. 2015 [46], the ovine fetus in the first third of pregnancy (around 50 dpc),  
133 expresses limited hepatic BPA glucuronidation activity, with an intrinsic clearance rate  
134 about 30-fold lower than in the last third of pregnancy.

135 In addition, the conjugation/deconjugation balance is clearly in favour of BPA-G  
136 deconjugation in ovine fetal gonads (ovaries and testes) with an activity of BPA-G  
137 hydrolysis 10-fold higher than the activity of BPA conjugation [46]. The possible

138 reactivation of BPA-G into BPA could contribute to an increased exposure of fetal  
139 sensitive tissues to bioactive BPA *in situ*.

140

141 In order to model the exposure conditions of the human fetus, we selected two  
142 concentrations to expose the ovine fetal ovaries in a culture model:  $3 \times 10^{-7}$  M (68.5  
143 ng/mL) and  $3 \times 10^{-5}$  M (6.85  $\mu$ g/mL). The lowest concentration corresponds to that  
144 measured in the biological fluids of human fetuses in the last third of pregnancy [44-  
145 45] and the higher concentration accounts for the low conjugation capacity of the fetal  
146 liver, the trapping of BPA-G at the fetal compartment and the capacity of the fetal  
147 gonads to deconjugate BPA-G.

148 We showed that initiation and progression of *ex-vivo* prophase I meiosis in sheep  
149 explants needed retinoic acid and that BPA is a potent meiotic toxicant altering  
150 expression of numerous genes involved in cell cycle transition, prophase I meiosis,  
151 and spindle formation. Therefore, exposure to BPA could affect the formation and  
152 differentiation of primordial follicles that would contain oocytes unable to complete  
153 prophase I.

154

155

156 **2. Materials and methods**

157

158 The experimental procedure is summarised in Fig. 1.

159

160 **2.1. Collection of fetal sheep gonads**

161

162 Procedures for handling sheep were conducted in compliance with the guidelines for  
163 Care and Use of Agricultural Animals in Agricultural Research and Teaching  
164 (authorization from local ethical committee CEEA n°45). All sheep fetuses were  
165 obtained from pregnant Pré-Alpes females, following hormonal treatment as previously  
166 described [7]. Sheep fetuses were collected at our local slaughterhouse (INRAE, Jouy  
167 en Josas, France) at 50, 60, 70 *dpc*. The genetic sex of all fetuses was determined by  
168 PCR amplification of the *SRY* and *ZFY/ZFX* genes using liver genomic DNA as  
169 previously described [7].

170

171 **2.2. Organ culture**

172

173 Each fetal ovary was cut into 2 pieces. Ovarian pieces were processed and cultured in  
174 Waymouth medium MB 752/1 supplemented with 25 mg/L pyruvic acid, sodium salt  
175 (Sigma, France), 1 ml/100ml of media of ITS+ (insulin, transferrin, and selenous acid;  
176 Becton Dickinson, France), 50 UI/ml penicillin, 50 µg/ml streptomycin (P433-Sigma-  
177 Aldrich). Ovarian pieces were rinsed in the culture medium and then transferred onto  
178 30-mm-diameter uncoated culture plate inserts (Millicell Cell Culture Insert, 0.4 µm  
179 pore size; Millipore SAS, France) in individual wells of a 6-well culture dish containing  
180 1.1mL of media. The cultures were incubated at 38.5 C in an incubator gassed with

181 5% CO<sub>2</sub> and 95% air. Cultures were equilibrated for 24 hours and then considered as  
182 day 0. On day 0, representative pieces of fetal ovaries were fixed in Bouin's liquid or  
183 flash frozen in liquid nitrogen and then stored at -80° C, to serve as non-cultured  
184 controls. Ovarian explants were then cultured for 10 or 20 days under various exposure  
185 conditions. The medium in each well was replaced daily. Retinoic acid (RA) 10<sup>-6</sup>M  
186 (R2625, Sigma-Aldrich) or AM580 10<sup>-6</sup> M (product number sc-203505, Tebu-bio,  
187 France) were added to cultures for 20 days or 7 days, respectively. The compound 4-  
188 (5,6,7,8-tetrahydro-5,5,8,8-tetramethyl-2-naphtamido) benzoic acid (AM580) is a  
189 synthetic stable analogue of retinoic acid (RA) that acts as a selective RAR $\alpha$  agonist  
190 and is resistant to CYP26 metabolism. For this last reason, AM580 was added only the  
191 first 7 days. In contrast, RA needs to be added continuously during all the culture period  
192 because it was rapidly degraded by endogenous CYP26 enzymes. Stock solutions of  
193 the various retinoids were prepared in dimethyl sulfoxide (DMSO, D2650-Sigma-  
194 Aldrich) under dimmed light and stored at -80 C and protected from light until use.

195

### 196 **2.3. Chemicals**

197

198 Bisphenol A (BPA, 4,4'-dihydroxy-2,2'-diphénylpropane) (N°CAS 80-05-7, Interchim)  
199 was dissolved in 0.01% dimethyl sulfoxide (DMSO, D2650-Sigma-Aldrich) and was  
200 added to culture medium for obtaining a final concentration of 3x10<sup>-5</sup> M (6.85 $\mu$ g/mL,  
201 BPA1) or 3x10<sup>-7</sup>M (68.48ng/mL, BPA2). Explants at 50 *dpc* were first cultured in control  
202 culture medium for 24 h (D0). Then the culture was pursued for 10 and 20 days,  
203 corresponding to 60 and 70 *dpc* with half of the wells added with BPA and the other  
204 half in basal medium (+DMSO only) to serve as controls.

205

## 206 **2.4. Histology**

207 For histological studies, fetal ovaries were fixed in Bouin's Solution. Fixed tissues were  
208 dehydrated, embedded in paraffin by standard procedures with a Citadel automat  
209 (Thermo Fisher Scientific - Shandon Citadel 1000) and cut into 5- $\mu$ m sections. Bouin-  
210 fixed sections were stained with haematoxylin and eosin (HES). Images were captured  
211 using a digital slide scanner (Hamamatsu Photonics, Massy, France) and images were  
212 analysed with NDP view software (Hamamatsu). As previously described [47], oogonia  
213 were identified as small cells with high nucleocytoplasmic ratio and the presence of  
214 prominent nucleoli.

215

## 216 **2.5. RNA extraction**

217

218 Total RNA from freshly explanted fetal ovaries or from cultured ovarian explant pieces  
219 were isolated using Trizol Reagent (Life Technologies, Paisley, UK), DNase-treated  
220 and purified with RNeasy Mini kit (Qiagen, Courtaboeuf, France) following the  
221 manufacturer's instructions. Total RNAs were quantified by Nanodrop ND-1000 UV  
222 measurement or by Qubit® Fluorometric Quantitation (Thermo Fisher Scientific,  
223 Illkirch, France) and the RNA integrity was verified using an Agilent 2100 Bioanalyser  
224 (Matriks, Norway). Only samples with RNA Integrity Number greater than 9 were used  
225 for quantitative PCR or microarray hybridizations.

226

## 227 **2.6. Real-time quantitative PCR**

228

229 In order to measure gene expression after the different condition cultures or exposures,  
230 reverse transcription was performed with the Thermo Scientific Kit Maxima First Strand

231 cDNA Synthesis Kit for RT-qPCR (Thermo Fisher Scientific, Illkirch, France) on each  
 232 extracted total RNA. Quantitative RT-PCR was performed using the Step One system  
 233 with Fast SYBR® Green Master Mix (Applied Biosystems, Courtaboeuf, France).  
 234 YWHAZ, HPRT1 and H2AFZ were used as reference genes for the comparative CT  
 235 method for relative quantitation of gene expression. Results were analysed using  
 236 qBase software (Biogazelle NV, Ghent, Belgium). The sequences of primers used for  
 237 qRT-PCR are presented in Table 1.

238

**Table 1:** Primer sequences used for qPCR.

Gene	Primers forward 5'-3'	Primers reverse 5'-3'
AURKA	GTGGAAGACGGACTCAGAGC	CACACAGGACTGGGAAGGTT
BUB1	CTCAGTGGCTTTTCGGACTGT	TGCGCTAAATCTGCTACACC
CDKN1	ATATGGGTCTGGGAGCTGTG	AGGATGCTACAGGAGCTGGA
CITED2	ACCGTTCTGGATCAGGAAAA	CCACTGACGACATTCCACAC
DMC1	TTGCGAAAAGGAAGAGGAGA	CCCAATTCCTCCAGCAGTTA
ESR1	CAGGTGCCCTATTACCTGGA	GCCACCTTGACGTCGATTAT
ESR2	GCCTCCATGATGATGTCCTT	CACTTGGTCGTACAGGCTGA
GPR30	AGGTGTTCAACCTGGACGAG	GAGGAAGAAGACGCTGCTGT
H2AFZ	GCGTATTACCCTCGTCACTTG	CAGCAATTGTAGCCTTGATGAGA
HPRT1	GAACGGCTGGCTCGAGATGT	TCCAACAGGTGGCAAAGAA
KIF18A	TTCCTTTTGTGTTTGTGCTTTTG	CCACCACACTGACTCAGGAA
NR2F1	TTCTTCGTCCGTTTGGTAGG	CCAAGGTCTAGGAGCACTGG
REC8	TGGTGGAGACTGACCTACCC	TCCACAGACATCATCCCAA

SPO11	TACCGAGGAGGAGTCTGCAT	GTTCACCTTGGTGCCATCTT
STRA8	CACCCCTGAGGAGATCCTTT	AGCACGGAAGTGGAGGCTAGA
SYCP1	CCCATGCTTGAACAGACTGA	GTCTGCTCATTGGCTCTGAA
TMEM167	TGCAGTGTGCTGTATCGTGA	GGCAGATCAGTCCCTTTTTG
TPX2	CTCCTGCCCGAGTGAATAAG	GTGCAAGGGGAACGTAGGTA
YWHAZ	GGAGCCCGTAGGTCATCTTG	CTCGAGCCATCTGCTGTTTTT

239

240 For each experiment, median values were plotted with GraphPad Prism, and statistical  
 241 analyses were performed with Kruskal-Wallis test in R software (Rcmdr package (p-  
 242 value<0.05) (p-value between 0.01 and 0.05 = \*\*, p-value less than 0.01 = \*\*\*).

243

## 244 **2.7. Customized ovine microarray hybridization**

245

246 Transcriptome analysis was conducted on a custom 15K Agilent oligo sheep  
 247 microarray previously described in [48]. Labelling and hybridization were performed at  
 248 the “Plate-forme Biopuces et Séquençage” (<http://genomeast.igbmc.fr/>). RNA integrity  
 249 and quantity was checked, respectively, by Bioanalyzer (Agilent) analysis and  
 250 Nanodrop ND-1000 UV measurement. Labelling and hybridisation were carried out  
 251 using the Quick Amp Labelling kit for one-color labeling (Agilent, 5190-0442) and the  
 252 One-Color RNA Spike-in Kit (Agilent, 5188–5282) according to the manufacturer’s  
 253 instructions with 200 ng of total RNAs starting quantities. Arrays were scanned with the  
 254 Agilent DNA Microarray Scanner Model G2565B and image analysis performed with  
 255 Agilent Feature Extraction software v9.5.3.1. In order to verify the quality and  
 256 hybridization reproducibility of the array, hybridisation tests with RNA from control  
 257 sheep ovaries were performed using one-color labelling and standard hybridization:



258 70–80% of spots were significantly hybridised and replicate experiments showed good  
259 reproducibility. For gene array, data processing and analysis were conducted using  
260 Bioconductor packages suite (<http://www.bioconductor.org/index.html>) and LIMMA  
261 package50 with the R statistical program. Raw median signal from Feature Extraction  
262 array files was used as non-processed signal and log2 transformed. Background was  
263 then subtracted locally, and intra-array normalisation performed by subtracting the  
264 array median signal from each spot signal on the same array. Multiple testing  
265 corrections were applied and differentially expressed probes were considered under a  
266 False Discovery Rate (FDR) of 5% [49].

267

## 268 **2.8. Gene ontology enrichment**

269

270 Differentially expressed probes were analysed with Gene Ontology (GO) and Kyoto  
271 Encyclopedia of Genes and Genomes (KEGG) pathway membership with Database  
272 performed using the DAVID Bioinformatic Database 6.8 (<https://david.ncifcrf.gov/>)  
273 [50,51]. These analyses and pathways were considered significant for a Benjamini  
274 corrected enrichment p-value of less than 0.05.

275

## 276 **3. Results**

277

### 278 **3.1. Initiation and progression of prophase I meiosis**

279

280 Newly explanted 50 *dpc* ovaries contained mitotic germ cells, some at pre-leptotene  
281 stages, many with prominent nucleoli (Fig. 2A-A). Germ cells at zygotene were  
282 observed at 60 *dpc* with the first diplotene stage germ cells seen at 70 *dpc* (Fig. 2A-B,  
283 2A-C). In order to better characterise the timing of meiosis initiation and progression,  
284 we analysed the expression of key meiotic markers: *STRA8*, *SYCP1*, *DMC1* and  
285 *SPO11* in freshly collected sheep fetal ovaries ranging from 50 to 70 *dpc* (Fig. 2B, C,  
286 D, E). Strikingly a 10-fold increase in *STRA8* mRNA (between 50 and 55 *dpc*) and a 4-  
287 fold increase in *SYCP1* mRNA (between 50 and 60 *dpc*) were observed in the sheep  
288 fetal ovary coincident with the onset of meiosis. In contrast to mouse, a lack of  
289 synchronicity in the expression of the various meiotic markers was observed, with  
290 *DMC1*, and *SCYP1* being expressed initially while *SPO11* was up-regulated from 70  
291 *dpc*.

292

293 Sheep fetal ovaries freshly isolated at 50 *dpc* were cultured for 10 or 20 days in culture  
294 medium with or without retinoic acid (RA  $10^{-6}$ M) or AM580 ( $10^{-6}$ M). When the fetal  
295 ovaries were cultured without retinoic supplementation (control), no features of meiosis  
296 were observed 20 days later and the germ cells remained in a proliferative state (Fig.  
297 3A). The addition of RA or AM580 enabled oogonia to enter meiosis (Fig. 3A). At 10  
298 and 20 days of culture RA- or AM580-supplemented fetal ovaries demonstrated a  
299 histologically normal appearance, containing germ cells and somatic cells similar to  
300 that in tissue from uncultured age-matched controls (Figs. 2&3). After 20 days of

301 culture with RA or AM580 germ cells in pachytene/diplotene and diplotene stages had  
302 appeared (Fig 3A). RA and AM580 up-regulated mRNA levels of meiotic markers,  
303 particularly, SYCP1, and SPO11 (Fig. 3B). However, the addition of  $10^{-6}$ M Am580  
304 during the first 7 days of culture yielded histological and transcriptional characteristics  
305 closest to those observed *ex-vivo* at 70 dpc and appeared more effective than RA itself  
306 (Figs 2, 3B).

307

### 308 **3.2. Effects of BPA on 20 day-exposed fetal explants**

309

#### 310 **BPA down-deregulates meiotic marker gene expression**

311 In order to determine whether prophase I meiosis is altered by BPA exposure in sheep  
312 fetal ovary explants, and which mechanisms were involved, we analysed mRNA  
313 expression of several candidate meiotic genes using qRT-PCR from gonads cultured  
314 in control (BPA-free+AM580+DMSO) conditions and after exposure to BPA  
315 concentrations. Following *in vitro* exposure to  $3 \times 10^{-7}$  M and  $3 \times 10^{-5}$  M BPA for 20 days,  
316 changes in mRNA levels of *STRA8*, *DMC1*, *REC8* and *SYCP1* occurred (Fig. 4).  
317 Meiotic gene expression levels were reduced at both BPA concentrations, except for  
318 *REC8* where only the highest BPA concentration led to a marked reduction in  
319 expression.

320

321 Control and BPA-exposed ovaries after 20 days of culture were then analysed using a  
322 custom sheep microarray containing 15K probes. After exposure to the lowest  
323 concentrations of BPA ( $3 \times 10^{-7}$  M), only 2 probes were significantly up-regulated (FDR  
324 5% or  $\text{adj-pval} < 0.05$ ) corresponding to Nuclear Receptor Subfamily 2 Group F Member  
325 1 (NR2F1) and transmembrane protein 167A (TMEM167A) transcripts (Table S1,

326 sheet #1). The protein encoded by NR2F1, is a nuclear hormone receptor and  
327 transcriptional regulator whereas TMEM167A is involved in constitutive secretory  
328 pathway. Both were also deregulated in the same manner with the highest  
329 concentration of BPA. Validation of these expression changes was performed by qRT-  
330 PCR. The results confirmed microarray data, especially at the highest concentration  
331 ( $10^{-5}$  M BPA). At the lowest concentration, only NR2F1 presented an up-regulation by  
332 RT-qPCR. (Fig. 6 A, B).

333

334 In contrast, after exposure to  $3 \times 10^{-5}$  M BPA, 446 probes were deregulated, 225 were  
335 down- and 221 were up-regulated with FDR 5% and threshold of  $\pm 0.7$  on the log2  
336 transformed fold change (Log2FC) and 677 probes were deregulated (259 down- and  
337 418 up-regulated) with FDR 5% and  $\text{Log2FC} < \pm 0.2$  (Table S1, sheet #2, Fig.5A).  
338 Among the down-regulated probes, many corresponded to transcripts expressed in  
339 pre-meiotic or meiotic female germ cells, such as BOULE (BOLL), DAZL and its targets  
340 TEX11, SMC1B and also TRIP13, RAD18, RAD51, MAD2L1 [52]. The expression of  
341 the meiosis gatekeeper STRA8 was also decreased. Two members of the doublesex  
342 and mab-3-related transcription factor family (DMRT) present in the fetal ovaries at the  
343 time of meiotic initiation, DMRTC2 (DMRT7) and DMRT1 are transcriptionally reduced.  
344 MAEL (Maelstrom), an evolutionarily conserved protein that interacts with other piRNA  
345 components to silencing of transposable elements was down-regulated after BPA  
346 exposure. In the same way, Topaz1 (Testis and Ovary-specific PAZ domain gene 1) a  
347 germ cell specific gene potentially involved in piRNA pathway was also reduced [16],  
348 as well as, MEIOB, which is specifically implicated in meiotic homologous  
349 recombination [53].

350

351 **BPA alters cell cycle regulation and spindle assembly pathways**

352 To further understand biological functions and pathways altered by BPA, the 677  
353 sheep differentially (adj pval<0.05 and Log2FC threshold  $\pm 0.2$ ) expressed probes  
354 (control *versus*  $3 \times 10^{-5}$  M BPA conditions) were functionally annotated based on Gene  
355 Ontology (GO) terms and Kyoto Encyclopedia of Genes and Genomes (KEGG)  
356 pathway through DAVID ontology database. Uncharacterised putative genes and  
357 redundant probes were removed before analyses. Overall, 516 official gene symbols  
358 were subjected to DAVID analyses. To increase the depth of genes with GO  
359 annotations, we used the *Homo Sapiens* genome annotation as background  
360 (recommended in [54], and obtained statistically enriched biological processes and  
361 molecular functions in which the proteins are involved. The transcripts were classified  
362 in the ontological categories: Biological process (BP), Cellular component (CC), and  
363 Molecular function (MF) (Table S2, Fig.5). It is important to note that an individual  
364 transcript could be represented in several categories.

365

366 GO enrichment analysis showed that the Top 10 of biological processes significantly  
367 enriched from differentially expressed genes following BPA exposure were: cell cycle  
368 (GO:0007049 & GO:0022402), organelle fission (GO:0048285), nuclear division  
369 (GO:0000280), mitotic nuclear division (GO:0007067), chromosome segregation  
370 (GO:0098813 & GO:0007059), mitotic cell cycle (GO:0000278 & GO:1903047), sister  
371 chromatid segregation (GO:0000819) and meiotic cell cycle (GO:0051321) (Fig. 5B).  
372 The associated Cellular Component GO terms were focused on chromosomes  
373 (condensed chromosome GO:0000793, centromeric region GO:0000775), kinetochore  
374 (GO:0000776) and spindle (GO:0005819). The most significant affected molecular  
375 functions were: macromolecular complex binding (GO:004487), chromatin binding

376 (GO:0003682) enzyme binding (GO:0019899) and identical protein binding  
377 (GO:0042802), (Fig. 5C and Table S2,). In accordance with GO analysis, the most  
378 significant terms of KEGG pathway analysis included Cell cycle (pvalue: 8.88E-04) and  
379 Oocyte meiosis (pValue: 0.04) (Fig.5D). In conclusion, Gene ontology (GO) and Kyoto  
380 Encyclopedia of Genes and Genomes (KEGG) enrichment analyses revealed that the  
381 majority of differentially expressed (BPA vs Control) were involved in specific biological  
382 process associated to gametogenesis, and specifically germ cell meiosis. (Fig. 5 and  
383 Table S2).

384

385 In order to confirm the deregulation of these pathways, selected genes were analysed  
386 by qRT-PCR. Among them, CDKN1A and CITED2, involved into the cell-cycle  
387 regulation, were both up-regulated in microarray analysis at the highest BPA  
388 concentration. qRT-PCR analysis confirmed response following exposure to  $10^{-5}$  M  
389 BPA only (Fig.6 C, D). KIF18A and BUB1B, two key factors of spindle assembly, were  
390 down-regulated in microarray and qRT-PCR analysis at  $10^{-5}$  M BPA (Fig.6 E, F). The  
391 same was observed for AURKA and TPX2: decreased expression in BPA exposed  
392 explants analysed by microarray and qRT-PCR (Fig.6 G, H).

393

394 **4. Discussion**

395 We have demonstrated, in a fetal ovine ovarian explant system recapitulating meiosis  
396 initiation and progression, that BPA disrupted fetal ovarian meiosis (prophase I). We  
397 showed that BPA caused at human-relevant doses, inhibition of meiosis I by affecting  
398 not only meiotic marker gene expression but also key factors involved in cell cycle  
399 transition and with spindle assembly, microtubule organizing centre and chromosome  
400 alignment and segregation. However, certain expression deregulations were only  
401 demonstrated at the highest dose of BPA ( $3 \times 10^{-5} \text{M}$ ). Validation by qRT-PCR revealed  
402 that the expression of several transcripts was significantly affected at the lowest dose  
403 ( $3 \times 10^{-7} \text{M}$ ), such STRA8, SYCP1, DMC1, SPO11, NR2F1, BUB1 and TPX2. This could  
404 be due to the lower sensitivity of the microarray technique that requires greater gene  
405 expression differentials than qRT-PCR. Moreover, BPA effects on meiosis could occur  
406 at different concentrations according to the mode of action, such as methylation  
407 changes of key regulator genes, disturbance of estrogen or retinoic acid signaling  
408 pathways. It is possible that each molecular process be sensitive to different BPA  
409 concentrations and that the highest dose recapitulates all the effects.

410

411 **4.1. Comparison between *in vivo* and *in vitro* ovary culture**

412

413 New approaches for *in vitro* prophase I meiotic toxicity testing are required in order to  
414 increase the number of molecules tested per animal, thus reducing animal numbers.  
415 Critical barriers to overcome included: (1) the maintenance of a coherent 3D structure  
416 in the explants, and (2) the development of *in vitro* culture conditions essential for  
417 entrance into meiosis and sustained progression of prophase I meiosis in species  
418 where these phenomena extend over several weeks, such as ruminants or humans.

419 To our knowledge, we showed here the first characterisation of a sheep fetal ovary  
420 explant model that allows the initiation and progression of prophase I meiosis *in vitro*  
421 in human developmentally-relevant animal model.

422

423 Meiotic commitment is a two-step process: (1) the acquisition of intrinsic factors  
424 enabling germ cells to initiate meiosis, notably through the expression of DAZL [55];  
425 (2) the reception of a meiosis-inducing signal that triggers STRA8 expression,  
426 ultimately leading to meiotic entry [13,14, 56-58]. Retinoic acid (RA) induces germ cells  
427 to express both STRA8, a gene required for meiotic initiation [59-65], and REC8, a  
428 gene required for meiotic progression [64]. In sheep, DAZL is expressed from 49 *dpc*  
429 and STRA8 expression in fetal ovaries is detected as early as 50 *dpc* with a peak at  
430 55 *dpc* followed by rising expression of meiotic genes like DMC1 and SYCP1, MSH4  
431 and MSH5 [7]. This time course of expression was confirmed here by qRT-PCR  
432 analysis of freshly explanted ovaries at 50, 55, 60 and 70 *dpc*.

433

434 In order to trigger prophase I meiosis, retinoids was added at 50 *dpc* when the oogonia  
435 become competent to receive the meiosis inducing factor following expression of  
436 DAZL. In cultures from 50 *dpc* supplemented with RA or its analogue AM580,  
437 expression profiles of STRA8, DMC1, SYCP1 and SPO11 were analogous to the  
438 corresponding *in vivo* developmental stages. The *in vitro* model of ovary explant culture  
439 described here, preserved tissue integrity and morphology and supported the survival  
440 of 50 *dpc* -ovary explants for over 3 weeks with appropriate development of the female  
441 germline. Moreover, 50 *dpc* -explants after 10 and 20 days of cultures were  
442 characterised by similar prophase I meiosis stages to those of freshly explanted  
443 ovaries at 60 and 70 *dpc* (*i.e.* pachytene and diplotene stages). The time course,



444 initiation and progression of meiosis were comparable to those of *in vivo* ovaries [7].  
445 Since the AM580 RA analogue induced results similar to those obtained with RA, the  
446 action of RA is likely mainly mediated by RAR $\alpha$ .

447

448 As in the human fetal ovary [12,13], no initiation and progression of meiosis was  
449 observed in sheep ovary explants cultured without RA, confirming that meiosis is not  
450 spontaneous in the sheep fetal ovary. In contrast, meiotic cells spontaneously appear  
451 in both mouse and rat fetal ovaries cultured for a few days in a defined culture medium  
452 (i.e. with no serum or retinoids for 3 or 4 days) [65].

453

#### 454 **4.2 Effects of BPA exposure on oocyte prophase I meiosis progression**

455

456 We focused on the effects of BPA on prophase I meiosis and the underlying molecular  
457 mechanisms. BPA decreased expression of STRA8, REC8, DMC1 and SYCP1 in  
458 exposed ovary explants after 20 days of culture (Fig. 4). This down-regulation of  
459 meiotic markers will necessarily have consequences for meiotic progression, either by  
460 non-initiation of prophase I, or by a process of delay or acceleration of the various  
461 stages. Further studies at intermediate culture durations (5, 10, 15 days) will be needed  
462 to decide between these possibilities. Several *in vitro/ex-vivo* systems have been  
463 developed to culture human fetal ovaries [33,66–68]. In humans, independently of the  
464 BPA concentration used (1, 5, 10, 20 and 30  $\mu$ M), BPA affects meiotic progression by  
465 increasing the proportion of oocytes at leptoneuma and reducing the proportion of  
466 oocytes that reach pachynema *in vitro* [33].

467

468 We showed by microarray analysis that  $3 \times 10^{-7}$  M BPA exposure affected expression  
469 of two genes, *TMEM167A* (transmembrane protein 167A) and *NR2F1* (nuclear  
470 receptor subfamily 2, group F, member 1, also called COUP-TF1 chicken ovalbumin  
471 upstream promoter transcription factor-1), which were up-regulated. *TMEM167A* is  
472 involved in the regulation of vesicular trafficking and contributes to aggressiveness of  
473 gliomas by deregulation of vesicle transport system [69,70], The presence of  
474 *TMEM167A* mRNA in fetal ovary is however confirmed by RNAseq data from fetal  
475 mouse ovary [71] (<https://rgv.genouest.org/>) [72] (Fig. S1A) and is also observed in  
476 human developing fetal ovaries from 6 to 17 PCW [73]. These data are presented in  
477 Figure S1B. Further investigations will be needed to determine its role in fetal ovary.

478

479 COUP-TFs are orphan receptors of the nuclear receptor superfamily. In human fetal  
480 ovaries, COUP-TF1 (*NR2F1*) was located to the cytoplasm of some oocytes and to the  
481 nuclei of scattered somatic cells in the second trimester (15 weeks) [74]. *COUP-TF1*  
482 transcript expression was significantly increased in human fetal ovary following  
483 endocrine disruption due to maternal smoking [74]. COUP-TF1 interacts with ER and  
484 ER ligand influences COUP-TF-ERE half-site binding [75]. It is therefore possible that  
485 the binding of BPA with ER could modify the interactions with COUP-TF1 and  
486 deregulate the COUP-TF-responsible target genes.

487 Several studies have suggested that COUP-TF could be part of retinoid signalling  
488 pathways both *in vivo* and in cell culture systems [76–79]. Moreover, the trend towards  
489 increased *NR2F1* may also disturb retinoic acid signalling [80], with potential disruption  
490 of meiosis entry. This agrees closely with our observations that increased *NR2F1* could  
491 be associated with deregulation of *STRA8* and consequently of numerous other  
492 meiosis-related genes following BPA exposure. COUP-TF1 appears as a master

493 regulator in several signalling pathways such as ER, AHR and RA signalling and its  
494 deregulation could broadly impact the fetal ovarian gene expression program.

495

### 496 **4.3 Biological Processes Impacted by BPA**

497

498 At the higher BPA ( $3 \times 10^{-5} \text{M}$ ) concentration, exposure dysregulated expression of  
499 numerous genes (677 probes) with 418 up- and 259 down-regulated probes. BPA-  
500 induced STRA8 deregulation via disturbance in RA signalling is likely contributory to  
501 many of these changes in gene expression. This is supported by recent studies in mice  
502 showing that STRA8 acts as a transcription factor and regulates the expression of  
503 thousands of genes including meiotic prophase genes, factors mediating DNA  
504 replication and the G1-S cell-cycle transition, and genes that promote the lengthy  
505 prophase unique to meiosis I [81]. Strikingly, these pathways involved in cell-cycle  
506 regulation were affected in our BPA-exposed ovary explant GO-term analysis.  
507 *CDKN1A* and *CITED2*, known to be associated with ovarian dysfunction and affecting  
508 both germ cells and somatic cells [90, 91], were amongst the up-regulated genes. Both  
509 presented a similar profile, increasing at the higher BPA concentration, first evidence  
510 that these are BPA target genes.

511 CDK inhibitor p21 (*CDKN1A* or p21) inhibits cell cycle progression by interacting with  
512 cyclin–CDK complexes and the expression of *Cdkn1a* (p21) normally decreases during  
513 the transition from mitosis to meiosis, as shown by single-cell RNA sequencing of early  
514 mouse female germ cells [82]. The observed up-regulation of *CDKN1A/p21* in our  
515 ovarian explants in response to BPA  $3 \times 10^{-5} \text{M}$  could therefore result into a blockage of  
516 mitosis/meiosis transition.

517 CITED2 (CBP/p300 interacting transactivator 2 with GLU/ASP-rich C terminal domain  
518 2), involved in oocyte development, is markedly increased at the initiation of oocyte  
519 growth in mouse primordial follicles [83]. Cited2 is also expressed in mouse and human  
520 cumulus cells [84,85] and high levels in these cells are associated with polycystic ovary  
521 syndrome [86] and diminished ovarian reserve in humans [84]. The observed increase  
522 in our BPA-exposed ovarian cultures could lead to similar phenotypes in adult female  
523 offspring.

524

525 Previous studies on BPA or BPS exposure during *in vitro* meiotic maturation (IVM) has  
526 shown an impairment of the progression to metaphase-II (MII) as well as disrupted  
527 meiotic spindle assembly and organization in mouse [28,29], porcine [87], bovine [88]  
528 and human [89] oocytes. Recently, Yang et al shown that a brief (4h) exposure of  
529 mouse ovulated oocytes to increasing concentrations (5, 25, 50 µg/ml) of BPA or BPF  
530 disrupted spindle organization in a dose-dependent manner. They identify a link  
531 between these microtubule defects and altered distribution of key spindle associated  
532 factors, as well as Aurora Kinase A activity. [90]. Our microarray transcriptomic  
533 analysis also revealed a decreased expression of multiple spindle-associated factors  
534 such as BUB1, Kinesin Family Member 18 and 23 (KIF18A & KIF23), TPX2 and also  
535 AURKA. Recently, Blengini et al. demonstrated that female oocyte-specific AURKA  
536 knockout mice are sterile, and their oocytes fail to complete meiosis I [91]. The  
537 microtubule-associated protein TPX2 is also a key mitotic regulator that contributes  
538 through distinct pathways to spindle assembly. TPX2 functions in the activation,  
539 stabilisation and spindle localisation of the Aurora-A kinase [92] while TPX2 expression  
540 in somatic cells exposed to BPA is also disrupted [93]. This is in agreement with our

541 data showing altered expression of factors essential for the assembly of the spindle  
542 after BPA exposure.

543

544 *BUB1B* encodes BUBR1, a crucial spindle assembly checkpoint (SAC) component  
545 involved in cell division [94-96]. The SAC is a safeguard mechanism to avoid premature  
546 chromosome segregation before correct kinetochore binding to the spindle. A strong  
547 reduction of BubR1 has been observed in oocytes of women approaching menopause  
548 and in ovaries of aged mice, which led to the hypothesis that a gradual decline of  
549 BubR1 contributes to age-related aneuploidization [97,98]. Exposure to 20µg/mL BPA  
550 of cumulus cells led to significantly decreased expression of BUB1B [99]. All these data  
551 reinforce our results showing BPA exposure induced a reduction of BUB1B expression  
552 that can lead to abnormal spindle assembly and chromosome mis-segregation.

553 Finally, Kif18a, a member of the kinesin-8 family, was found to be expressed in mouse  
554 oocytes, being closely associated with microtubules [100] and Kif18a knock down  
555 caused the failure of first polar body extrusion, resulting in severe chromosome  
556 misalignment. [100]. The decrease of kif18A in our 10<sup>-5</sup> M BPA-exposed cultures could  
557 also contribute to spindle disorganisation.

558 It is remarkable that several gene deregulations observed following BPA exposure of  
559 adult follicles containing oocytes II were also found in our study. This implies that some  
560 molecular mechanisms impacted in adult and fetal models are shared. However, the  
561 disruption of the early stages of meiosis can generate more drastic effects because  
562 the alteration of the ovarian reserve can lead to premature ovarian failure and infertility.  
563 Indeed, this reserve built up during fetal life is not renewed during the reproductive life  
564 of female mammals.

565

## 566 **5. Conclusion**

567

568 We have developed a culture model enabling initiation and maintenance of prophase  
569 I meiosis *in vitro* in sheep fetal ovary explants. Cultured oogonia in these explants  
570 followed the same pattern of gene expression changes as seen in non-cultured fetal  
571 oogonia of matching ages. This is important since mono-ovulatory sheep represents a  
572 physiologically human-relevant model for testing ovary toxicity of endocrine disruptor  
573 exposures during fetal life. Our results show that BPA exposure affects oogenesis in  
574 fetal sheep ovary, disrupting the meiotic process via three different pathways. Some of  
575 these deregulations are also found in the process of late meiosis that takes place in  
576 oocytes II in adults (spindle assembly). The other two altered processes  
577 (mitosis/meiosis transition and prophase I) are specific to fetal stages.

578 Importantly, such meiotic changes induced during these fetal stages would decrease  
579 the ovarian reserve and increase the frequency of chromosomally abnormal oocytes  
580 (aneuploidy) both leading to sub or infertility in the adult female. There are multiple  
581 underlying mechanisms and BPA could act either by interfering with the RA pathway  
582 and disturbing STRA8 action and/or via the ER pathway by controlling cell-cycle  
583 progression. Overall, our findings provide novel insight regarding the multiple effects  
584 of BPA exposure on fetal oogonia that go beyond deregulation of factors directly  
585 involved in meiotic recombination by also disrupting meiotic spindle organization as  
586 well as the mitosis / meiosis transition.

587

## 588 **Conflict of interest statement**

589 The authors declare that they have no known competing financial interests or personal  
590 relationships that could have appeared to influence the work reported in this paper.

591

592 **Acknowledgements**

593 This work was supported by funding to PAF and CC from the Wellcome Trust (080388)  
594 and the European Community's Seventh Framework Programme under grant  
595 agreement no. 212885. (<http://www.abdn.ac.uk/reef/>).

596

597 The authors would like to thank INRAE, SAAJ, experimental animal facility (Sciences  
598 de l'Animal et de l'Aliment de Jouy), especially Jean-Pierre Albert, Didier Mauchand,  
599 and Jean-François Alkombre.

600

601 **References**

- 602 [1] A.-A. Chassot, F. Ranc, E.P. Gregoire, H.L. Roepers-Gajadien, M.M. Taketo, G. Camerino, D.G. de  
603 Rooij, A. Schedl, M.-C. Chaboissier, Activation of beta-catenin signaling by Rspo1 controls  
604 differentiation of the mammalian ovary, *Hum. Mol. Genet.* 17 (2008) 1264–1277.  
605 <https://doi.org/10.1093/hmg/ddn016>.
- 606 [2] B. Nicol, S.A. Grimm, A. Gruzdev, G.J. Scott, M.K. Ray, H.H.-C. Yao, Genome-wide identification  
607 of FOXL2 binding and characterization of FOXL2 feminizing action in the fetal gonads, *Hum.*  
608 *Mol. Genet.* 27 (2018) 4273–4287. <https://doi.org/10.1093/hmg/ddy312>.
- 609 [3] C. Ottolenghi, S. Omari, J.E. Garcia-Ortiz, M. Uda, L. Crisponi, A. Forabosco, G. Pilia, D.  
610 Schlessinger, Foxl2 is required for commitment to ovary differentiation, *Hum. Mol. Genet.* 14  
611 (2005) 2053–2062. <https://doi.org/10.1093/hmg/ddi210>.
- 612 [4] M. Pannetier, A.-A. Chassot, M.-C. Chaboissier, E. Pailhoux, Involvement of FOXL2 and RSPO1 in  
613 Ovarian Determination, Development, and Maintenance in Mammals, *Sex. Dev. Genet. Mol.*  
614 *Biol. Evol. Endocrinol. Embryol. Pathol. Sex Determ. Differ.* 10 (2016) 167–184.  
615 <https://doi.org/10.1159/000448667>.
- 616 [5] N.H. Uhlenhaut, S. Jakob, K. Anlag, T. Eisenberger, R. Sekido, J. Kress, A.-C. Treier, C. Klugmann,  
617 C. Klasen, N.I. Holter, D. Riethmacher, G. Schütz, A.J. Cooney, R. Lovell-Badge, M. Treier,  
618 Somatic sex reprogramming of adult ovaries to testes by FOXL2 ablation, *Cell.* 139 (2009) 1130–  
619 1142. <https://doi.org/10.1016/j.cell.2009.11.021>.
- 620 [6] K. Duffin, R. a. L. Bayne, A.J. Childs, C. Collins, R.A. Anderson, The forkhead transcription factor  
621 FOXL2 is expressed in somatic cells of the human ovary prior to follicle formation, *Mol. Hum.*  
622 *Reprod.* 15 (2009) 771–777. <https://doi.org/10.1093/molehr/gap065>.
- 623 [7] B. Mandon-Pépin, A. Oustry-Vaiman, B. Vigier, F. Piumi, E. Cribiu, C. Cotinot, Expression profiles  
624 and chromosomal localization of genes controlling meiosis and follicular development in the  
625 sheep ovary, *Biol. Reprod.* 68 (2003) 985–995. <https://doi.org/10.1095/biolreprod.102.008557>.
- 626 [8] M. Pannetier, S. Fabre, F. Batista, A. Kocer, L. Renault, G. Jolivet, B. Mandon-Pépin, C. Cotinot,  
627 R. Veitia, E. Pailhoux, FOXL2 activates P450 aromatase gene transcription: towards a better  
628 characterization of the early steps of mammalian ovarian development, *J. Mol. Endocrinol.* 36  
629 (2006) 399–413. <https://doi.org/10.1677/jme.1.01947>.
- 630 [9] A.-A. Chassot, I. Gillot, M.-C. Chaboissier, R-spondin1, WNT4, and the CTNNB1 signaling  
631 pathway: strict control over ovarian differentiation, *Reprod. Camb. Engl.* 148 (2014) R97-110.  
632 <https://doi.org/10.1530/REP-14-0177>.
- 633 [10] M. De Felici, F.G. Klinger, D. Farini, M.L. Scaldaferrri, S. Iona, M. Lobascio, Establishment of  
634 oocyte population in the fetal ovary: primordial germ cell proliferation and oocyte programmed  
635 cell death, *Reprod. Biomed. Online.* 10 (2005) 182–191. [https://doi.org/10.1016/s1472-](https://doi.org/10.1016/s1472-6483(10)60939-x)  
636 [6483\(10\)60939-x](https://doi.org/10.1016/s1472-6483(10)60939-x).
- 637 [11] G. Jolivet, N. Daniel-Carlier, E. Harscoët, E. Airaud, A. Dewaele, C. Pierson, F. Giton, L.  
638 Boulanger, N. Daniel, B. Mandon-Pépin, M. Pannetier, E. Pailhoux, Fetal estrogens are not  
639 involved in sex determination but critical for early ovarian differentiation in rabbits,  
640 *Endocrinology.* (2021) bqab210. <https://doi.org/10.1210/endocr/bqab210>.
- 641 [12] A. Jørgensen, J.E. Nielsen, S. Perlman, L. Lundvall, R.T. Mitchell, A. Juul, E. Rajpert-De Meyts, Ex  
642 vivo culture of human fetal gonads: manipulation of meiosis signalling by retinoic acid  
643 treatment disrupts testis development, *Hum. Reprod. Oxf. Engl.* 30 (2015) 2351–2363.  
644 <https://doi.org/10.1093/humrep/dev194>.
- 645 [13] R. Le Bouffant, M.J. Guerquin, C. Duquenne, N. Frydman, H. Coffigny, V. Rouiller-Fabre, R.  
646 Frydman, R. Habert, G. Livera, Meiosis initiation in the human ovary requires intrinsic retinoic  
647 acid synthesis, *Hum. Reprod. Oxf. Engl.* 25 (2010) 2579–2590.  
648 <https://doi.org/10.1093/humrep/deq195>.
- 649 [14] A.J. Childs, G. Cowan, H.L. Kinnell, R.A. Anderson, P.T.K. Saunders, Retinoic Acid signalling and  
650 the control of meiotic entry in the human fetal gonad, *PLoS One.* 6 (2011) e20249.  
651 <https://doi.org/10.1371/journal.pone.0020249>.



- 652 [15] A. Jørgensen, J.E. Nielsen, M. Blomberg Jensen, N. Græm, E. Rajpert-De Meyts, Analysis of  
653 meiosis regulators in human gonads: a sexually dimorphic spatio-temporal expression pattern  
654 suggests involvement of DMRT1 in meiotic entry, *Mol. Hum. Reprod.* 18 (2012) 523–534.  
655 <https://doi.org/10.1093/molehr/gas030>.
- 656 [16] A. Baillet, R. Le Bouffant, J.N. Volff, A. Luangpraseuth, E. Poumerol, D. Thépot, E. Pailhoux, G.  
657 Livera, C. Cotinot, B. Mandon-Pépin, TOPAZ1, a novel germ cell-specific expressed gene  
658 conserved during evolution across vertebrates, *PloS One.* 6 (2011) e26950.  
659 <https://doi.org/10.1371/journal.pone.0026950>.
- 660 [17] K.P. McNatty, P. Smith, N.L. Hudson, D.A. Heath, D.J. Tisdall, W.S. O, R. Braw-Tal, Development  
661 of the sheep ovary during fetal and early neonatal life and the effect of fecundity genes, *J.*  
662 *Reprod. Fertil. Suppl.* 49 (1995) 123–135.
- 663 [18] P. Smith, D. Wilhelm, R.J. Rodgers, Development of mammalian ovary, *J. Endocrinol.* 221 (2014)  
664 R145–161. <https://doi.org/10.1530/JOE-14-0062>.
- 665 [19] P. Smith, W.S. O, N.L. Hudson, L. Shaw, D.A. Heath, L. Condell, D.J. Phillips, K.P. McNatty, Effects  
666 of the Booroola gene (FecB) on body weight, ovarian development and hormone  
667 concentrations during fetal life, *J. Reprod. Fertil.* 98 (1993) 41–54.  
668 <https://doi.org/10.1530/jrf.0.0980041>.
- 669 [20] T.L. Greco, A.H. Payne, Ontogeny of expression of the genes for steroidogenic enzymes P450  
670 side-chain cleavage, 3 beta-hydroxysteroid dehydrogenase, P450 17 alpha-hydroxylase/C17-20  
671 lyase, and P450 aromatase in fetal mouse gonads, *Endocrinology.* 135 (1994) 262–268.  
672 <https://doi.org/10.1210/endo.135.1.8013361>.
- 673 [21] P.A. Fowler, R.A. Anderson, P.T. Saunders, H. Kinnell, J.I. Mason, D.B. Evans, S. Bhattacharya, S.  
674 Flannigan, S. Franks, A. Monteiro, P.J. O’Shaughnessy, Development of steroid signaling  
675 pathways during primordial follicle formation in the human fetal ovary, *J. Clin. Endocrinol.*  
676 *Metab.* 96 (2011) 1754–1762. <https://doi.org/10.1210/jc.2010-2618>.
- 677 [22] F.W. George, J.D. Wilson, Conversion of androgen to estrogen by the human fetal ovary, *J. Clin.*  
678 *Endocrinol. Metab.* 47 (1978) 550–555. <https://doi.org/10.1210/jcem-47-3-550>.
- 679 [23] S. Lun, P. Smith, T. Lundy, A. O’Connell, N. Hudson, K.P. McNatty, Steroid contents of and  
680 steroidogenesis in vitro by the developing gonad and mesonephros around sexual  
681 differentiation in fetal sheep, *J. Reprod. Fertil.* 114 (1998) 131–139.  
682 <https://doi.org/10.1530/jrf.0.1140131>.
- 683 [24] P. MAULEON, J. BEZARD, M. TERQUI, Very early and transient 17  $\beta$ -estradiol secretion by fetal  
684 sheep ovary. In vitro study, *Ann. Biol. Anim. Biochim. Biophys.* 17 (1977) 399–401.
- 685 [25] J.P. Weniger, Aromatase activity in fetal gonads of mammals, *J. Dev. Physiol.* 14 (1990) 303–  
686 306.
- 687 [26] L.N. Vandenberg, R. Hauser, M. Marcus, N. Olea, W.V. Welshons, Human exposure to bisphenol  
688 A (BPA), *Reprod. Toxicol. Elmsford N.* 24 (2007) 139–177.  
689 <https://doi.org/10.1016/j.reprotox.2007.07.010>.
- 690 [27] Z.R. Craig, W. Wang, J.A. Flaws, Endocrine-disrupting chemicals in ovarian function: effects on  
691 steroidogenesis, metabolism and nuclear receptor signaling, *Reprod. Camb. Engl.* 142 (2011)  
692 633–646. <https://doi.org/10.1530/REP-11-0136>.
- 693 [28] A. Can, O. Semiz, O. Cinar, Bisphenol-A induces cell cycle delay and alters centrosome and  
694 spindle microtubular organization in oocytes during meiosis, *Mol. Hum. Reprod.* 11 (2005) 389–  
695 396. <https://doi.org/10.1093/molehr/gah179>.
- 696 [29] U. Eichenlaub-Ritter, E. Vogt, S. Cukurcam, F. Sun, F. Pacchierotti, J. Parry, Exposure of mouse  
697 oocytes to bisphenol A causes meiotic arrest but not aneuploidy, *Mutat. Res.* 651 (2008) 82–92.  
698 <https://doi.org/10.1016/j.mrgentox.2007.10.014>.
- 699 [30] P.A. Hunt, K.E. Koehler, M. Susiarjo, C.A. Hodges, A. Ilagan, R.C. Voigt, S. Thomas, B.F. Thomas,  
700 T.J. Hassold, Bisphenol A exposure causes meiotic aneuploidy in the female mouse, *Curr. Biol.*  
701 *CB.* 13 (2003) 546–553. [https://doi.org/10.1016/s0960-9822\(03\)00189-1](https://doi.org/10.1016/s0960-9822(03)00189-1).

- 702 [31] S. Lenie, R. Cortvrindt, U. Eichenlaub-Ritter, J. Smitz, Continuous exposure to bisphenol A during  
703 in vitro follicular development induces meiotic abnormalities, *Mutat. Res.* 651 (2008) 71–81.  
704 <https://doi.org/10.1016/j.mrgentox.2007.10.017>.
- 705 [32] A. Mlynarcíková, E. Nagyová, M. Ficková, S. Scsuková, Effects of selected endocrine disruptors  
706 on meiotic maturation, cumulus expansion, synthesis of hyaluronan and progesterone by  
707 porcine oocyte-cumulus complexes, *Toxicol. Vitro Int. J. Publ. Assoc. BIBRA.* 23 (2009) 371–377.  
708 <https://doi.org/10.1016/j.tiv.2008.12.017>.
- 709 [33] M.A. Brieño-Enríquez, P. Robles, N. Camats-Tarruella, R. García-Cruz, I. Roig, L. Cabero, F.  
710 Martínez, M.G. Caldés, Human meiotic progression and recombination are affected by  
711 Bisphenol A exposure during in vitro human oocyte development, *Hum. Reprod. Oxf. Engl.* 26  
712 (2011) 2807–2818. <https://doi.org/10.1093/humrep/der249>.
- 713 [34] T. Corbel, V. Gayrard, C. Viguié, S. Puel, M.Z. Lacroix, P.-L. Toutain, N. Picard-Hagen, Bisphenol A  
714 disposition in the sheep maternal-placental-fetal unit: mechanisms determining fetal internal  
715 exposure, *Biol. Reprod.* 89 (2013) 11. <https://doi.org/10.1095/biolreprod.112.106369>.
- 716 [35] G. Gauderat, N. Picard-Hagen, P.-L. Toutain, T. Corbel, C. Viguié, S. Puel, M.Z. Lacroix, P.  
717 Mindeguia, A. Bousquet-Melou, V. Gayrard, Bisphenol A glucuronide deconjugation is a  
718 determining factor of fetal exposure to bisphenol A, *Environ. Int.* 86 (2016) 52–59.  
719 <https://doi.org/10.1016/j.envint.2015.10.006>.
- 720 [36] G. Gauderat, N. Picard-Hagen, P.-L. Toutain, R. Servien, C. Viguié, S. Puel, M.Z. Lacroix, T.  
721 Corbel, A. Bousquet-Melou, V. Gayrard, Prediction of human prenatal exposure to bisphenol A  
722 and bisphenol A glucuronide from an ovine semi-physiological toxicokinetic model, *Sci. Rep.* 7  
723 (2017) 15330. <https://doi.org/10.1038/s41598-017-15646-5>.
- 724 [37] C. Mantzouki, D. Bliatka, P.K. Iliadou, A. Margeli, I. Papassotiriou, G. Mastorakos, E. Kousta, D.G.  
725 Goulis, Serum Bisphenol A concentrations in men with idiopathic infertility, *Food Chem. Toxicol.*  
726 *Int. J. Publ. Br. Ind. Biol. Res. Assoc.* 125 (2019) 562–565.  
727 <https://doi.org/10.1016/j.fct.2019.02.016>.
- 728 [38] E. Salamanca-Fernández, M. Rodríguez-Barranco, J.P. Arrebola, F. Vela, C. Díaz, M.D. Chirlaque,  
729 S. Colorado-Yohar, A. Jiménez-Zabala, A. Irizar, M. Guevara, E. Ardanaz, L.M. Iribarne-Durán, J.  
730 Pérez Del Palacio, N. Olea, A. Agudo, M.-J. Sánchez, Bisphenol-A in the European Prospective  
731 Investigation into Cancer and Nutrition cohort in Spain: Levels at recruitment and associated  
732 dietary factors, *Environ. Res.* 182 (2020) 109012.  
733 <https://doi.org/10.1016/j.envres.2019.109012>.
- 734 [39] A. Aris, Estimation of bisphenol A (BPA) concentrations in pregnant women, fetuses and  
735 nonpregnant women in Eastern Townships of Canada, *Reprod. Toxicol. Elmsford N.* 45 (2014)  
736 8–13. <https://doi.org/10.1016/j.reprotox.2013.12.006>.
- 737 [40] M. Chen, A.G. Edlow, T. Lin, N.A. Smith, T.F. McElrath, C. Lu, Determination of bisphenol-A  
738 levels in human amniotic fluid samples by liquid chromatography coupled with mass  
739 spectrometry, *J. Sep. Sci.* 34 (2011) 1648–1655. <https://doi.org/10.1002/jssc.201100152>.
- 740 [41] A.G. Edlow, M. Chen, N.A. Smith, C. Lu, T.F. McElrath, Fetal bisphenol A exposure:  
741 concentration of conjugated and unconjugated bisphenol A in amniotic fluid in the second and  
742 third trimesters, *Reprod. Toxicol. Elmsford N.* 34 (2012) 1–7.  
743 <https://doi.org/10.1016/j.reprotox.2012.03.009>.
- 744 [42] M. Zbucka-Krętowska, U. Łazarek, W. Milyk, I. Sidorkiewicz, P. Pierzyński, R. Milewski, S.  
745 Wołczyński, J. Czerniecki, Simultaneous analysis of bisphenol A fractions in maternal and fetal  
746 compartments in early second trimester of pregnancy, *J. Perinat. Med.* 47 (2019) 765–770.  
747 <https://doi.org/10.1515/jpm-2019-0040>.
- 748 [43] R.R. Gerona, T.J. Woodruff, C.A. Dickenson, J. Pan, J.M. Schwartz, S. Sen, M.W. Friesen, V.Y.  
749 Fujimoto, P.A. Hunt, Bisphenol-A (BPA), BPA glucuronide, and BPA sulfate in midgestation  
750 umbilical cord serum in a northern and central California population, *Environ. Sci. Technol.* 47  
751 (2013) 12477–12485. <https://doi.org/10.1021/es402764d>.
- 752 [44] J. Lee, K. Choi, J. Park, H.-B. Moon, G. Choi, J.J. Lee, E. Suh, H.-J. Kim, S.-H. Eun, G.-H. Kim, G.J.  
753 Cho, S.K. Kim, S. Kim, S.Y. Kim, S. Kim, S. Eom, S. Choi, Y.D. Kim, S. Kim, Bisphenol A distribution

754 in serum, urine, placenta, breast milk, and umbilical cord serum in a birth panel of mother-  
755 neonate pairs, *Sci. Total Environ.* 626 (2018) 1494–1501.  
756 <https://doi.org/10.1016/j.scitotenv.2017.10.042>.

757 [45] B. Zhang, Y. He, H. Zhu, X. Huang, X. Bai, K. Kannan, T. Zhang, Concentrations of bisphenol A and  
758 its alternatives in paired maternal-fetal urine, serum and amniotic fluid from an e-waste  
759 dismantling area in China, *Environ. Int.* 136 (2020) 105407.  
760 <https://doi.org/10.1016/j.envint.2019.105407>.

761 [46] T. Corbel, E. Perdu, V. Gayraud, S. Puel, M.Z. Lacroix, C. Viguié, P.-L. Toutain, D. Zalko, N. Picard-  
762 Hagen, Conjugation and deconjugation reactions within the fetoplacental compartment in a  
763 sheep model: a key factor determining bisphenol A fetal exposure, *Drug Metab. Dispos. Biol.*  
764 *Fate Chem.* 43 (2015) 467–476. <https://doi.org/10.1124/dmd.114.061291>.

765 [47] L.F. Kurilo, Oogenesis in antenatal development in man, *Hum. Genet.* 57 (1981) 86–92.  
766 <https://doi.org/10.1007/BF00271175>.

767 [48] R.G. Lea, M.R. Amezcaga, B. Loup, B. Mandon-Pépin, A. Stefansdottir, P. Filis, C. Kyle, Z. Zhang, C.  
768 Allen, L. Purdie, L. Jouneau, C. Cotinot, S.M. Rhind, K.D. Sinclair, P.A. Fowler, The fetal ovary  
769 exhibits temporal sensitivity to a “real-life” mixture of environmental chemicals, *Sci. Rep.* 6  
770 (2016) 22279. <https://doi.org/10.1038/srep22279>.

771 [49] Y. Benjamini, Y. Hochberg, Controlling the False Discovery Rate: A Practical and Powerful  
772 Approach to Multiple Testing, *J. R. Stat. Soc. Ser. B Methodol.* 57 (1995) 289–300.

773 [50] D.W. Huang, B.T. Sherman, R.A. Lempicki, Bioinformatics enrichment tools: paths toward the  
774 comprehensive functional analysis of large gene lists, *Nucleic Acids Res.* 37 (2009) 1–13.  
775 <https://doi.org/10.1093/nar/gkn923>.

776 [51] D.W. Huang, B.T. Sherman, R.A. Lempicki, Systematic and integrative analysis of large gene lists  
777 using DAVID bioinformatics resources, *Nat. Protoc.* 4 (2009) 44–57.  
778 <https://doi.org/10.1038/nprot.2008.211>.

779 [52] R. Rosario, R.W.P. Smith, I.R. Adams, R.A. Anderson, RNA immunoprecipitation identifies novel  
780 targets of DAZL in human foetal ovary, *Mol. Hum. Reprod.* 23 (2017) 177–186.  
781 <https://doi.org/10.1093/molehr/gax004>.

782 [53] B. Souquet, E. Abby, R. Hervé, F. Finsterbusch, S. Tourpin, R. Le Bouffant, C. Duquenne, S.  
783 Messiaen, E. Martini, J. Bernardino-Sgherri, A. Toth, R. Habert, G. Livera, MEIOB targets single-  
784 strand DNA and is necessary for meiotic recombination, *PLoS Genet.* 9 (2013) e1003784.  
785 <https://doi.org/10.1371/journal.pgen.1003784>.

786 [54] M. Ha, M. Sabherwal, E. Duncan, S. Stevens, P. Stockwell, M. McConnell, A.E.-D. Bekhit, A.  
787 Carne, In-Depth Characterization of Sheep (*Ovis aries*) Milk Whey Proteome and Comparison  
788 with Cow (*Bos taurus*), *PloS One.* 10 (2015) e0139774.  
789 <https://doi.org/10.1371/journal.pone.0139774>.

790 [55] H.-A. Pan, R.-W. Liao, C.-L. Chung, Y.-N. Teng, Y.-M. Lin, P.-L. Kuo, DAZL protein expression in  
791 mouse preimplantation embryo, *Fertil. Steril.* 89 (2008) 1324–1327.  
792 <https://doi.org/10.1016/j.fertnstert.2007.03.041>.

793 [56] J. Bowles, D. Knight, C. Smith, D. Wilhelm, J. Richman, S. Mamiya, K. Yashiro, K.  
794 Chawengsaksophak, M.J. Wilson, J. Rossant, H. Hamada, P. Koopman, Retinoid signaling  
795 determines germ cell fate in mice, *Science.* 312 (2006) 596–600.  
796 <https://doi.org/10.1126/science.1125691>.

797 [57] J. Bowles, P. Koopman, Sex determination in mammalian germ cells: extrinsic versus intrinsic  
798 factors, *Reprod. Camb. Engl.* 139 (2010) 943–958. <https://doi.org/10.1530/REP-10-0075>.

799 [58] J. Koubova, D.B. Menke, Q. Zhou, B. Capel, M.D. Griswold, D.C. Page, Retinoic acid regulates  
800 sex-specific timing of meiotic initiation in mice, *Proc. Natl. Acad. Sci. U. S. A.* 103 (2006) 2474–  
801 2479. <https://doi.org/10.1073/pnas.0510813103>.

802 [59] G. MacLean, H. Li, D. Metzger, P. Chambon, M. Petkovich, Apoptotic extinction of germ cells in  
803 testes of *Cyp26b1* knockout mice, *Endocrinology.* 148 (2007) 4560–4567.  
804 <https://doi.org/10.1210/en.2007-0492>.

- 805 [60] H. Mu, J. Wu, H. Zhu, N. Li, F. Tang, X. Yao, C. Yang, S. Peng, G. Li, J. Hua, The function of Msx1  
806 gene in promoting meiosis of dairy goat male germline stem cells (mGSCs), *Cell Biochem. Funct.*  
807 31 (2013) 629–635. <https://doi.org/10.1002/cbf.3010>.
- 808 [61] K. Ohta, Y. Lin, N. Hogg, M. Yamamoto, Y. Yamazaki, Direct effects of retinoic acid on entry of  
809 fetal male germ cells into meiosis in mice, *Biol. Reprod.* 83 (2010) 1056–1063.  
810 <https://doi.org/10.1095/biolreprod.110.085787>.
- 811 [62] M. Tedesco, M.G. Desimio, F.G. Klinger, M. De Felici, D. Farini, Minimal concentrations of  
812 retinoic acid induce stimulation by retinoic acid 8 and promote entry into meiosis in isolated  
813 pregonadal and gonadal mouse primordial germ cells, *Biol. Reprod.* 88 (2013) 145.  
814 <https://doi.org/10.1095/biolreprod.112.106526>.
- 815 [63] E. Trautmann, M.-J. Guerquin, C. Duquenne, J.-B. Lahaye, R. Habert, G. Livera, Retinoic acid  
816 prevents germ cell mitotic arrest in mouse fetal testes, *Cell Cycle Georget. Tex.* 7 (2008) 656–  
817 664. <https://doi.org/10.4161/cc.7.5.5482>.
- 818 [64] J. Koubova, Y.-C. Hu, T. Bhattacharyya, Y.Q.S. Soh, M.E. Gill, M.L. Goodheart, C.A. Hogarth, M.D.  
819 Griswold, D.C. Page, Retinoic acid activates two pathways required for meiosis in mice, *PLoS*  
820 *Genet.* 10 (2014) e1004541. <https://doi.org/10.1371/journal.pgen.1004541>.
- 821 [65] G. Livera, V. Rouiller-Fabre, J. Valla, R. Habert, Effects of retinoids on the meiosis in the fetal rat  
822 ovary in culture, *Mol. Cell. Endocrinol.* 165 (2000) 225–231. [https://doi.org/10.1016/s0303-7207\(00\)00271-9](https://doi.org/10.1016/s0303-7207(00)00271-9).
- 824 [66] R.A. Anderson, L. McIlwain, S. Coutts, H.L. Kinnell, P.A. Fowler, A.J. Childs, Activation of the aryl  
825 hydrocarbon receptor by a component of cigarette smoke reduces germ cell proliferation in the  
826 human fetal ovary, *Mol. Hum. Reprod.* 21 (2015) 753. <https://doi.org/10.1093/molehr/gav044>.
- 827 [67] M.A. Briño-Enríquez, R. Reig-Viader, L. Cabero, N. Toran, F. Martínez, I. Roig, M. Garcia Caldes,  
828 Gene expression is altered after bisphenol A exposure in human fetal oocytes in vitro, *Mol.*  
829 *Hum. Reprod.* 18 (2012) 171–183. <https://doi.org/10.1093/molehr/gar074>.
- 830 [68] J.A. Stanley, J.A. Arosh, R.C. Burghardt, S.K. Banu, A fetal whole ovarian culture model for the  
831 evaluation of CrVI-induced developmental toxicity during germ cell nest breakdown, *Toxicol.*  
832 *Appl. Pharmacol.* 289 (2015) 58–69. <https://doi.org/10.1016/j.taap.2015.09.002>.
- 833 [69] M. Portela, B. Segura-Collar, I. Argudo, A. Sáiz, R. Gargini, P. Sánchez-Gómez, S. Casas-Tintó,  
834 Oncogenic dependence of glioma cells on kish/TMEM167A regulation of vesicular trafficking,  
835 *Glia.* 67 (2019) 404–417. <https://doi.org/10.1002/glia.23551>.
- 836 [70] B. Segura-Collar, R. Gargini, E. Tovar-Ambel, E. Hernández-SanMiguel, C. Epifano, I. Pérez de  
837 Castro, A. Hernández-Laín, S. Casas-Tintó, P. Sánchez-Gómez, The EGFR-TMEM167A-p53 Axis  
838 Defines the Aggressiveness of Gliomas, *Cancers.* 12 (2020).  
839 <https://doi.org/10.3390/cancers12010208>.
- 840 [71] L. Zhao, C. Wang, M.L. Lehman, M. He, J. An, T. Svingen, C.M. Spiller, E.T. Ng, C.C. Nelson, P.  
841 Koopman, Transcriptomic analysis of mRNA expression and alternative splicing during mouse  
842 sex determination, *Mol. Cell. Endocrinol.* 478 (2018) 84–96.  
843 <https://doi.org/10.1016/j.mce.2018.07.010>.
- 844 [72] T.A. Darde, O. Sallou, E. Becker, B. Evrard, C. Monjeaud, Y. Le Bras, B. Jégou, O. Collin, A.D.  
845 Rolland, F. Chalmel, The ReproGenomics Viewer: an integrative cross-species toolbox for the  
846 reproductive science community, *Nucleic Acids Res.* 43 (2015) W109-116.  
847 <https://doi.org/10.1093/nar/gkv345>.
- 848 [73] E. Lecluze, A.D. Rolland, P. Filis, B. Evrard, S. Leverrier-Penna, M.B. Maamar, I. Coiffec, V.  
849 Lavoué, P.A. Fowler, S. Mazaud-Guittot, B. Jégou, F. Chalmel, Dynamics of the transcriptional  
850 landscape during human fetal testis and ovary development, *Hum. Reprod. Oxf. Engl.* 35 (2020)  
851 1099–1119. <https://doi.org/10.1093/humrep/deaa041>.
- 852 [74] P.A. Fowler, A.J. Childs, F. Courant, A. MacKenzie, S.M. Rhind, J.-P. Antignac, B. Le Bizec, P. Filis,  
853 F. Evans, S. Flannigan, A. Maheshwari, S. Bhattacharya, A. Monteiro, R.A. Anderson, P.J.  
854 O’Shaughnessy, In utero exposure to cigarette smoke dysregulates human fetal ovarian  
855 developmental signalling, *Hum. Reprod. Oxf. Engl.* 29 (2014) 1471–1489.  
856 <https://doi.org/10.1093/humrep/deu117>.

- 857 [75] C.M. Klinge, Role of estrogen receptor ligand and estrogen response element sequence on  
858 interaction with chicken ovalbumin upstream promoter transcription factor (COUP-TF), *J.*  
859 *Steroid Biochem. Mol. Biol.* 71 (1999) 1–19. [https://doi.org/10.1016/s0960-0760\(99\)00124-7](https://doi.org/10.1016/s0960-0760(99)00124-7).
- 860 [76] K. Brubaker, M. McMillan, T. Neuman, H.O. Nornes, All-trans retinoic acid affects the  
861 expression of orphan receptors COUP-TF I and COUP-TF II in the developing neural tube, *Brain*  
862 *Res. Dev. Brain Res.* 93 (1996) 198–202. [https://doi.org/10.1016/0165-3806\(96\)00007-7](https://doi.org/10.1016/0165-3806(96)00007-7).
- 863 [77] A. Fjose, U. Weber, M. Mlodzik, A novel vertebrate svp-related nuclear receptor is expressed as  
864 a step gradient in developing rhombomeres and is affected by retinoic acid, *Mech. Dev.* 52  
865 (1995) 233–246. [https://doi.org/10.1016/0925-4773\(95\)00404-o](https://doi.org/10.1016/0925-4773(95)00404-o).
- 866 [78] L.J. Jonk, M.E. de Jonge, J.M. Vervaart, S. Wissink, W. Kruijer, Isolation and developmental  
867 expression of retinoic-acid-induced genes, *Dev. Biol.* 161 (1994) 604–614.  
868 <https://doi.org/10.1006/dbio.1994.1056>.
- 869 [79] J. van der Wees, P.J. Matharu, K. de Roos, O.H. Destrée, S.F. Godsave, A.J. Durston, G.E.  
870 Sweeney, Developmental expression and differential regulation by retinoic acid of *Xenopus*  
871 COUP-TF-A and COUP-TF-B, *Mech. Dev.* 54 (1996) 173–184. [https://doi.org/10.1016/0925-4773\(95\)00471-8](https://doi.org/10.1016/0925-4773(95)00471-8).
- 872 [80] Y. Zhuang, L.J. Gudas, Overexpression of COUP-TF1 in murine embryonic stem cells reduces  
873 retinoic acid-associated growth arrest and increases extraembryonic endoderm gene  
874 expression, *Differ. Res. Biol. Divers.* 76 (2008) 760–771. <https://doi.org/10.1111/j.1432-0436.2007.00258.x>.
- 875 [81] M.L. Kojima, D.G. de Rooij, D.C. Page, Amplification of a broad transcriptional program by a  
876 common factor triggers the meiotic cell cycle in mice, *ELife.* 8 (2019).  
877 <https://doi.org/10.7554/eLife.43738>.
- 878 [82] Z.-H. Zhao, J.-Y. Ma, T.-G. Meng, Z.-B. Wang, W. Yue, Q. Zhou, S. Li, X. Feng, Y. Hou, H. Schatten,  
879 X.-H. Ou, Q.-Y. Sun, Single-cell RNA sequencing reveals the landscape of early female germ cell  
880 development, *FASEB J. Off. Publ. Fed. Am. Soc. Exp. Biol.* 34 (2020) 12634–12645.  
881 <https://doi.org/10.1096/fj.202001034RR>.
- 882 [83] H. Pan, M.J. O'brien, K. Wigglesworth, J.J. Eppig, R.M. Schultz, Transcript profiling during mouse  
883 oocyte development and the effect of gonadotropin priming and development in vitro, *Dev.*  
884 *Biol.* 286 (2005) 493–506. <https://doi.org/10.1016/j.ydbio.2005.08.023>.
- 885 [84] P. May-Panloup, V. Ferré-L'Hôtelier, C. Morinière, C. Marcaillou, S. Lemerle, M.-C. Malinge, A.  
886 Coutolleau, N. Lucas, P. Reynier, P. Descamps, P. Guardiola, Molecular characterization of  
887 corona radiata cells from patients with diminished ovarian reserve using microarray and  
888 microfluidic-based gene expression profiling, *Hum. Reprod. Oxf. Engl.* 27 (2012) 829–843.  
889 <https://doi.org/10.1093/humrep/der431>.
- 890 [85] G. Vigone, V. Merico, A. Prigione, F. Mulas, L. Sacchi, M. Gabetta, R. Bellazzi, C.A. Redi, G.  
891 Mazzini, J. Adjaye, S. Garagna, M. Zuccotti, Transcriptome based identification of mouse  
892 cumulus cell markers that predict the developmental competence of their enclosed antral  
893 oocytes, *BMC Genomics.* 14 (2013) 380. <https://doi.org/10.1186/1471-2164-14-380>.
- 894 [86] Y. Fang, W. Shang, D.-L. Wei, S.-M. Zeng, Cited2 protein level in cumulus cells is a biomarker for  
895 human embryo quality and pregnancy outcome in one in vitro fertilization cycle, *Fertil. Steril.*  
896 105 (2016) 1351-1359.e4. <https://doi.org/10.1016/j.fertnstert.2015.12.137>.
- 897 [87] T. Žalmanová, K. Hošková, J. Nevoral, K. Adámková, T. Kott, M. Šulc, Z. Kotíková, Š. Prokešová, F.  
898 Jílek, M. Králíčková, J. Petr, Bisphenol S negatively affects the meiotic maturation of pig oocytes,  
899 *Sci. Rep.* 7 (2017) 485. <https://doi.org/10.1038/s41598-017-00570-5>.
- 900 [88] K.A. Campen, K.M. Kucharczyk, B. Bogin, J.M. Ehrlich, C.M.H. Combelles, Spindle abnormalities  
901 and chromosome misalignment in bovine oocytes after exposure to low doses of bisphenol A or  
902 bisphenol S, *Hum. Reprod. Oxf. Engl.* 33 (2018) 895–904.  
903 <https://doi.org/10.1093/humrep/dey050>.
- 904 [89] R. Machtinger, C.M.H. Combelles, S.A. Missmer, K.F. Correia, P. Williams, R. Hauser, C.  
905 Racowsky, Bisphenol-A and human oocyte maturation in vitro, *Hum. Reprod. Oxf. Engl.* 28  
906 (2013) 2735–2745. <https://doi.org/10.1093/humrep/det312>.
- 907  
908

- 909 [90] L. Yang, C. Baumann, R. De La Fuente, M.M. Viveiros, Mechanisms underlying disruption of  
910 oocyte spindle stability by bisphenol compounds, *Reprod. Camb. Engl.* 159 (2020) 383–396.  
911 <https://doi.org/10.1530/REP-19-0494>.
- 912 [91] C.S. Blengini, P. Ibrahimian, M. Vaskovicova, D. Drutovic, P. Solc, K. Schindler, Aurora kinase A is  
913 essential for meiosis in mouse oocytes, *PLoS Genet.* 17 (2021) e1009327.  
914 <https://doi.org/10.1371/journal.pgen.1009327>.
- 915 [92] R. Zhang, J. Roostalu, T. Surrey, E. Nogales, Structural insight into TPX2-stimulated microtubule  
916 assembly, *ELife.* 6 (2017) e30959. <https://doi.org/10.7554/eLife.30959>.
- 917 [93] S. Kim, D. Gwon, J.A. Kim, H. Choi, C.-Y. Jang, Bisphenol A disrupts mitotic progression via  
918 disturbing spindle attachment to kinetochore and centriole duplication in cancer cell lines,  
919 *Toxicol. Vitro Int. J. Publ. Assoc. BIBRA.* 59 (2019) 115–125.  
920 <https://doi.org/10.1016/j.tiv.2019.04.009>.
- 921 [94] L. Wei, X.-W. Liang, Q.-H. Zhang, M. Li, J. Yuan, S. Li, S.-C. Sun, Y.-C. Ouyang, H. Schatten, Q.-Y.  
922 Sun, BubR1 is a spindle assembly checkpoint protein regulating meiotic cell cycle progression of  
923 mouse oocyte, *Cell Cycle Georget. Tex.* 9 (2010) 1112–1121.  
924 <https://doi.org/10.4161/cc.9.6.10957>.
- 925 [95] S.A. Touati, E. Buffin, D. Cladière, K. Hached, C. Rachez, J.M. van Deursen, K. Wassmann, Mouse  
926 oocytes depend on BubR1 for proper chromosome segregation but not for prophase I arrest,  
927 *Nat. Commun.* 6 (2015) 6946. <https://doi.org/10.1038/ncomms7946>.
- 928 [96] R.E. Karess, K. Wassmann, Z. Rahmani, New insights into the role of BubR1 in mitosis and  
929 beyond, *Int. Rev. Cell Mol. Biol.* 306 (2013) 223–273. <https://doi.org/10.1016/B978-0-12-407694-5.00006-7>.
- 930
- 931 [97] M.A.J. Smits, G.E. Janssens, M. Goddijn, G. Hamer, R.H. Houtkooper, S. Mastenbroek, Longevity  
932 pathways are associated with human ovarian ageing, *Hum. Reprod. Open.* 2021 (2021)  
933 hoab020. <https://doi.org/10.1093/hropen/hoab020>.
- 934 [98] J. Lagirand-Cantaloube, C. Ciabrini, S. Charrasse, A. Ferrieres, A. Castro, T. Anahory, T. Lorca,  
935 Loss of Centromere Cohesion in Aneuploid Human Oocytes Correlates with Decreased  
936 Kinetochore Localization of the Sac Proteins Bub1 and Bubr1, *Sci. Rep.* 7 (2017) 44001.  
937 <https://doi.org/10.1038/srep44001>.
- 938 [99] A. Mansur, M. Adir, C. Racowsky, C.M. Combelles, N. Landa, R. Machtiger, Susceptibility of  
939 human cumulus cells to bisphenol a In vitro, *Reprod. Toxicol. Elmsford N.* 74 (2017) 189–194.  
940 <https://doi.org/10.1016/j.reprotox.2017.09.008>.
- 941 [100] F. Tang, M.-H. Pan, X. Wan, Y. Lu, Y. Zhang, S.-C. Sun, Kif18a regulates Sirt2-mediated tubulin  
942 acetylation for spindle organization during mouse oocyte meiosis, *Cell Div.* 13 (2018) 9.  
943 <https://doi.org/10.1186/s13008-018-0042-4>.
- 944

## Figure Legends

945

946

947 Figure 1: Schematic description of the experimental procedure.

948 Fetal ovaries were collected at 50 days *post coitum* (*dpc*), cut widthways into ~2 mm  
949 pieces (2 pieces/ovary) and one piece treated for histological analysis while the other  
950 was cultured. Three pieces from different fetuses were placed in each well. Cultures  
951 were incubated at 38.5C for up to 7 or 20 days with retinoids (RA or AM580) under a  
952 humidified atmosphere of 95% air and 5% CO<sub>2</sub>. The medium was replaced with fresh  
953 media after the first 24 h (D0) and then every 24 h. Explants were exposed to  
954 treatments on D0 by adding either vehicle at a final concentration of 0.1% v/v (dimethyl  
955 sulfoxide; DMSO) or BPA (0.3 or 30 μM). At the end of cultures, the explants were  
956 snap-frozen on dry ice and stored at -80C. Subsequently RNA extraction was  
957 performed, and RNA samples were analysed either by qRT-PCR or microarray.

958

959 Figure 2: Prophase I meiosis in sheep fetal ovary occurs between 55 *dpc* and 70*dpc*.

960 A timeline of ovine ovarian development is shown at the top of the figure. The key  
961 stages of prophase I of meiosis are illustrated at the bottom of the figure.

962 A-A) At culture onset, the 50 *dpc* fetal ovaries contained numerous mitotically active  
963 oogonia and some pre-leptotene and leptotene (L) oocytes had appeared. A-B) In 60  
964 *dpc* ovary explants, numerous oocytes had reached the zygotene stage (Z). A-C) 70  
965 *dpc*-ovary explants contained meiotic germ cells at different stages of prophase I,  
966 diplotene oocytes had appeared but pachytene (P) and zygotene are still present.

967 Transcript expression of *STRA8* (B), *DMC1* (C), *SYCP1* (D) and *SPO11* (E) was  
968 determined using qRT-PCR from in vivo fetal ovaries collected at 50, 55, 60 and 70  
969 *dpc*. Each stage corresponded to 5-6 ovary fragments, except day 55 that contained

970 only 2 fragments of uncultured ovaries. Gene expression values were normalized  
971 relative to *YWHAZ*, *HPRT1* and *H2AFZ* reference genes. Statistical analyses were  
972 performed with Kruskal-Wallis test in R software (Rcmdr package) (\*\* =  $p < 0.05$  and  
973 \*\*\*  $p < 0.01$ ).

974

975 Figure 3: Retinoids (RA & AM580) initiate entry and progression of meiosis prophase I  
976 in fetal ovary explant cultures.

977 A- Histological observations of explants of sheep fetal ovaries from 50 dpc cultured  
978 with  $10^{-6}$  M RA or AM580 or without (CTR) for 20 days. Black arrows indicate oogonia  
979 and oocytes in hematoxylin/eosin stained sections. In controls, germ cells were mainly  
980 in meiotic proliferation (black arrows show preleptotene stages). In contrast when  
981 explants were cultured with retinoids (AM580 or RA), oocytes initiated and progressed  
982 into prophase I meiotic stages, arrows indicated oocytes in pachytene or diplotene.

983 B- mRNA expression of meiosis regulators in explants cultured with  $10^{-6}$  M RA or  
984 AM580 or without (CTR) for 20 days. RNA was extracted, reverse transcribed and  
985 analysed by qRT-PCR. Transcript expression of *STRA8* (A), *DMC1* (B), *SYCP1* (C)  
986 and *SPO11* (D) was determined from 2-6 ovary explants according to presence of RA  
987 (circled in dotted lines, n=6), or AM580 (circled in full line, n=2). Cultures in control  
988 conditions contained 3 explants. Gene expression values were normalized relative to  
989 *YWHAZ*, *HPRT1* and *H2AFZ* reference genes. Statistical analyses were performed  
990 with Kruskal-Wallis test in R software (Rcmdr package) (\*\* =  $pval < 0.05$  and \*\*\*  $pval <$   
991  $0.01$ ).

992

993 Figure 4: Downregulation of meiosis marker expression in explant cultures exposed to  
994 BPA



995 Explants of sheep fetal ovaries at 50 dpc were cultured with  $10^{-6}$  M AM580 (CTR 20d)  
996 and exposed at 2 concentrations of BPA (0.3 $\mu$ M and 30 $\mu$ M) for 20 days. RNA was  
997 extracted, reverse transcribed and analysed by qRT-PCR. Transcript expression of  
998 *STRA8* (A), *DMC1* (B), *SYCP1* (C) *SPO11* (D) and *REC8* (E) was determined from 6  
999 control and 2 exposed ovary explants. Gene expression values were normalized  
1000 relative to *YWHAZ*, *HPRT1* and *H2AFZ* reference genes.

1001

1002 Figure 5: Deregulation of gene expression and alteration of cell cycle processes by  
1003 30  $\mu$ M BPA exposure

1004 (A) Number of differential probes according to their fold change. Only probes that met  
1005 an FDR of 5% (or adj-pval<0.05) and a threshold of  $\pm 0.2$  on the log<sub>2</sub>-transformed fold  
1006 change (LogFC) are displayed and represented according to their positive (shades of  
1007 yellow) or negative (shades of blue) fold change. 677 differentially expressed probes  
1008 were identified after 20 days of exposure to 30 $\mu$ M BPA versus control medium  
1009 (AM580+DMSO).

1010 (B-D) Among these 677 probes, 516 are known and unique official gene symbols were  
1011 obtained and submitted to DAVID analyses. Their biological significance was explored  
1012 by GO term enrichment analysis (DAVID) including biological process (B), molecular  
1013 function (C) and cellular component (D). Gene ontology (GO) analysis revealed that  
1014 cell cycle, cell proliferation, cell death processes and reproduction were the most  
1015 enriched biological processes (B); nucleotide and small molecule binding pathways,  
1016 the most enriched molecular functions (C) and nucleoplasm, microtubules cytoskeleton  
1017 and chromosomes, the most affected cellular components (D).

1018

1019 Figure 6: Validation by qRT-PCR of expression deregulation of 8 genes following  
1020 BPA exposure  
1021 After 20 days of culture, explants exposed to BPA (0.3 or 30  $\mu$ M) or not (CTR 20d)  
1022 were analysed by qRT-PCR. Transcript expression of *NR2F1*(A), *TMEM167* (B),  
1023 *CDKN1* (C), *CITED2* (D), *Kif18A* (E), *BUB1* (F), *AURKA* (G) and *TPX2* (H) was  
1024 determined from 3 control and 2 exposed ovary explants at both BPA concentrations.  
1025 Gene expression values were normalized relative to *YWHAZ*, *HPRT1* and *H2AFZ*  
1026 reference genes.

1027

## 1028 **Supplementary material**

1029

1030 Figure S1 *TREM167* expression in mouse and human fetal ovary

1031 (A) TPM-normalized average expression levels from mouse fetal ovary (pink) or  
1032 testis (light blue) (from 10.5 to 13.5 *dpc*, days postcoitum) according to the data of  
1033 Zhao et al. [65].

1034 (B) FPKM-normalized average expression levels from human fetal ovary (red) or  
1035 testis (blue) (from 6 to 17 PCW, postconceptional weeks; e7: early 7 PCW; l7: late  
1036 7 PCW) according to the data of Lecluze et al. [67].

1037

1038 Table S1:

1039 sheet 1\_ Fetal ovarian genes altered by 0.3 $\mu$ M BPA in *in vitro* culture

1040 sheet2\_ Fetal ovarian genes altered by 30 $\mu$ M BPA in *in vitro* culture

1041

1042 Table S2: Functional annotation of differentially expressed probes

1043

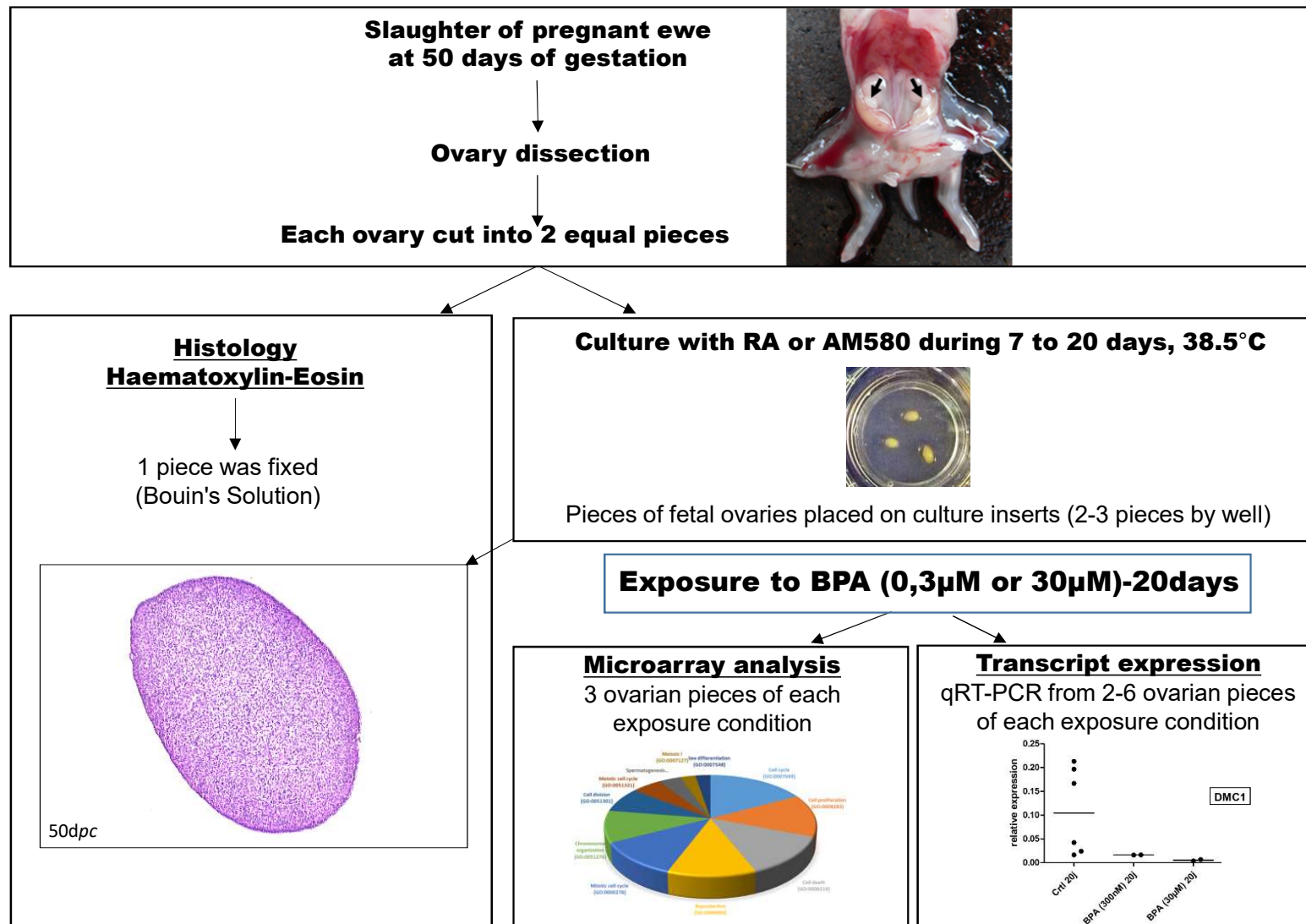
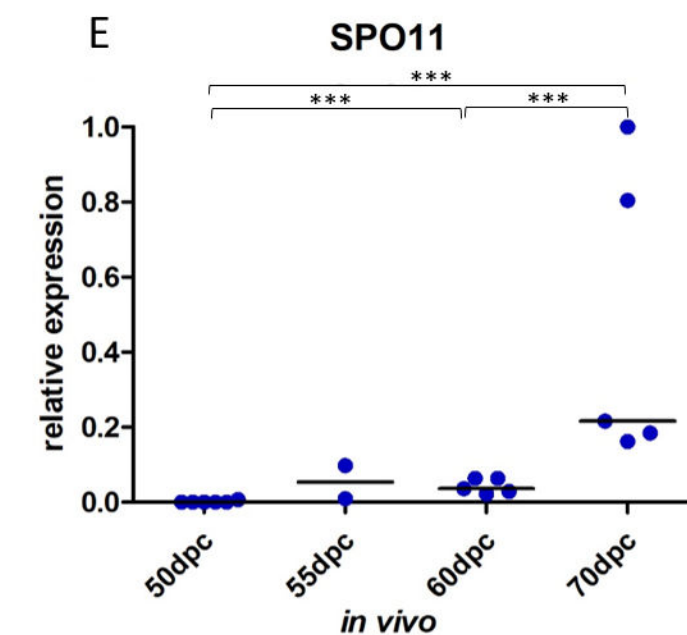
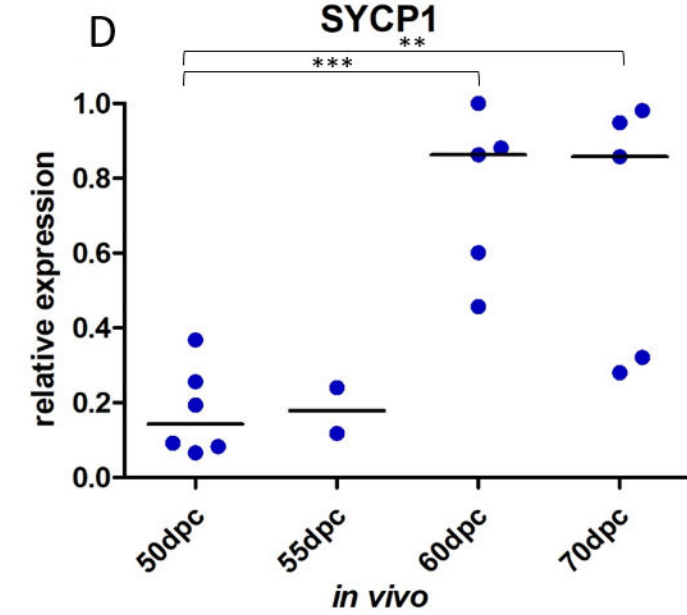
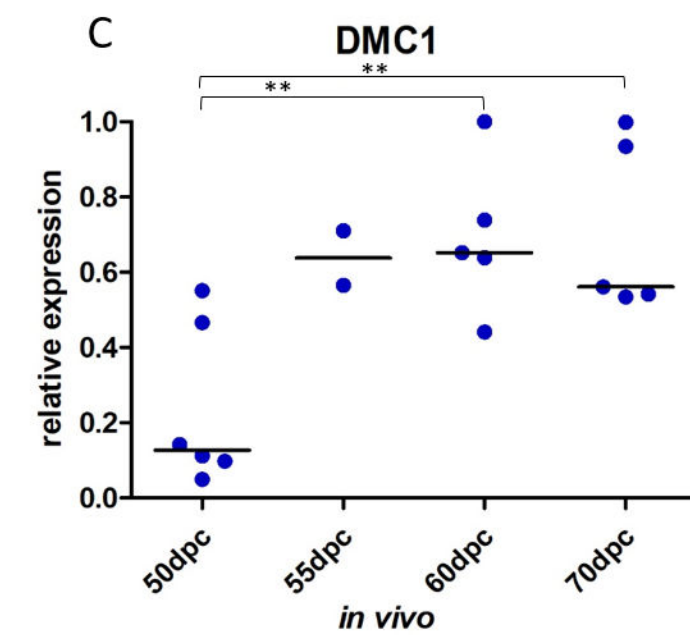
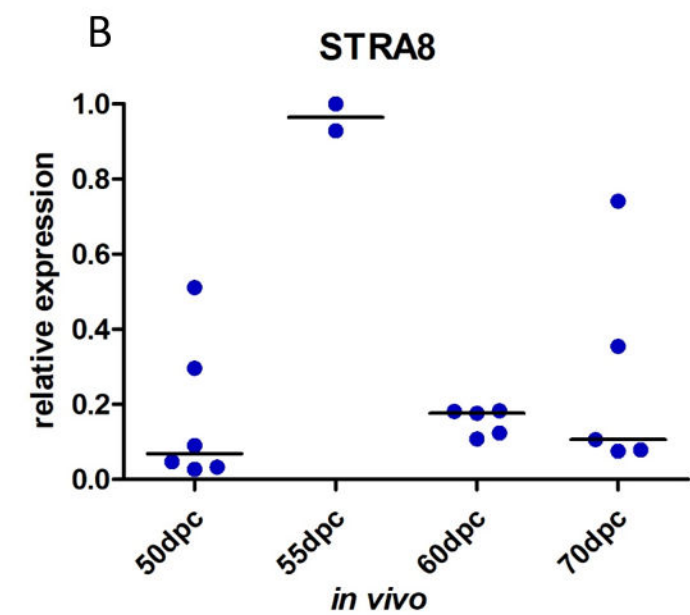
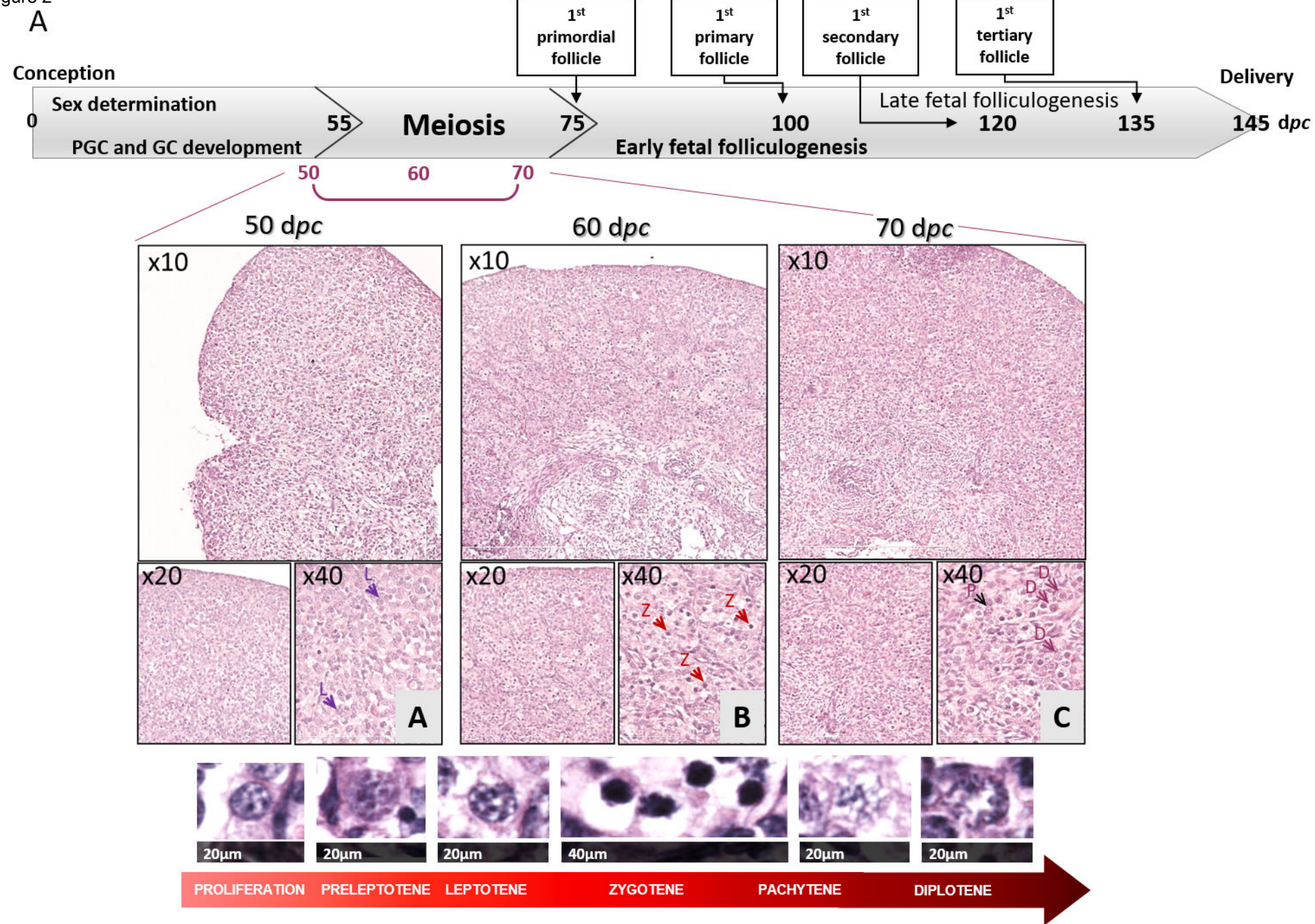
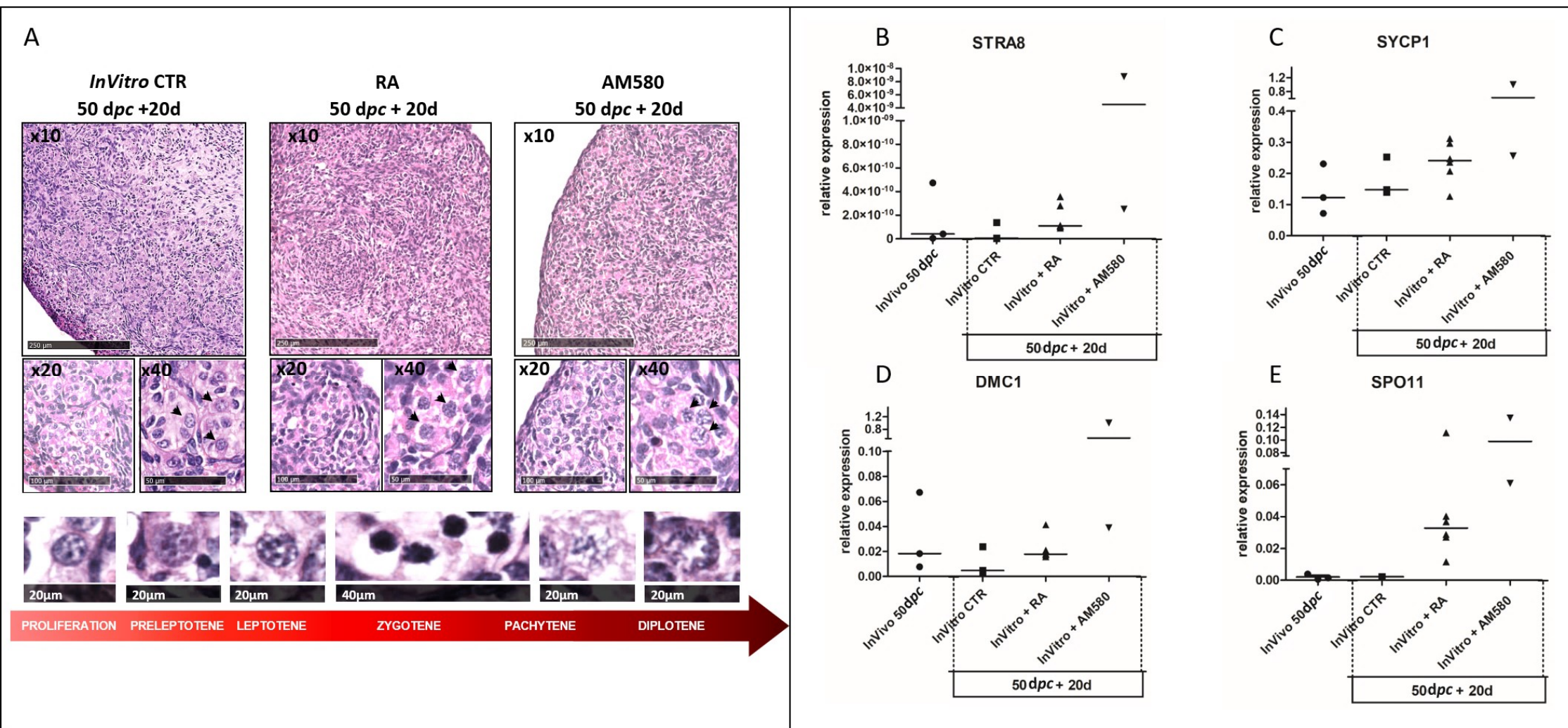


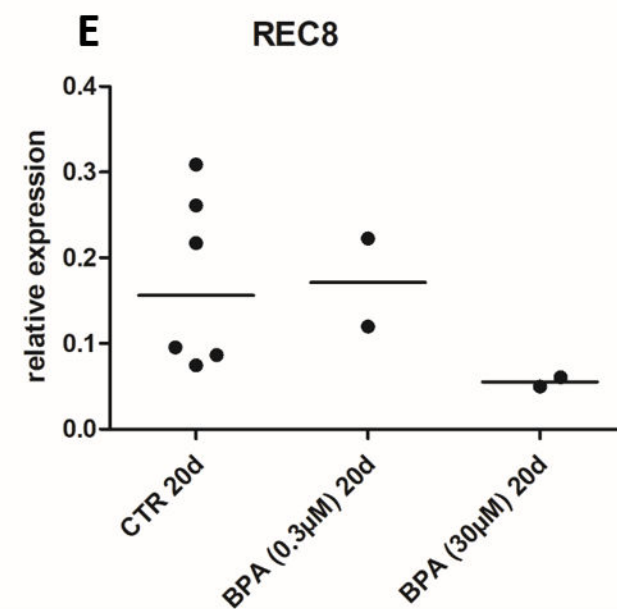
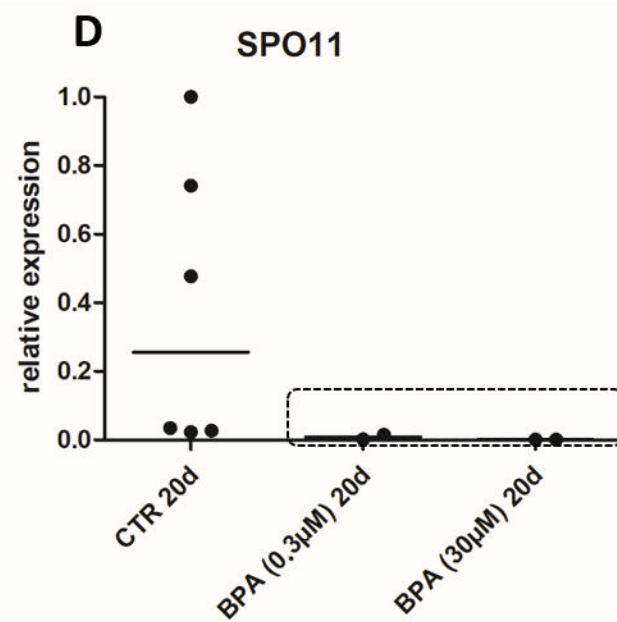
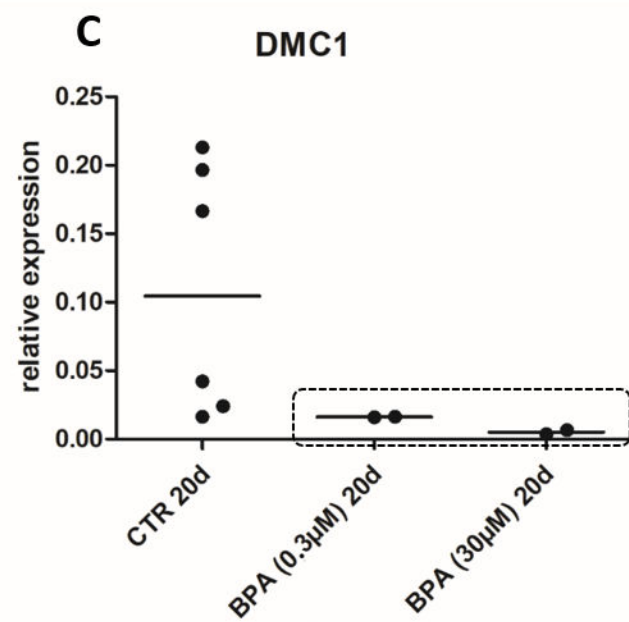
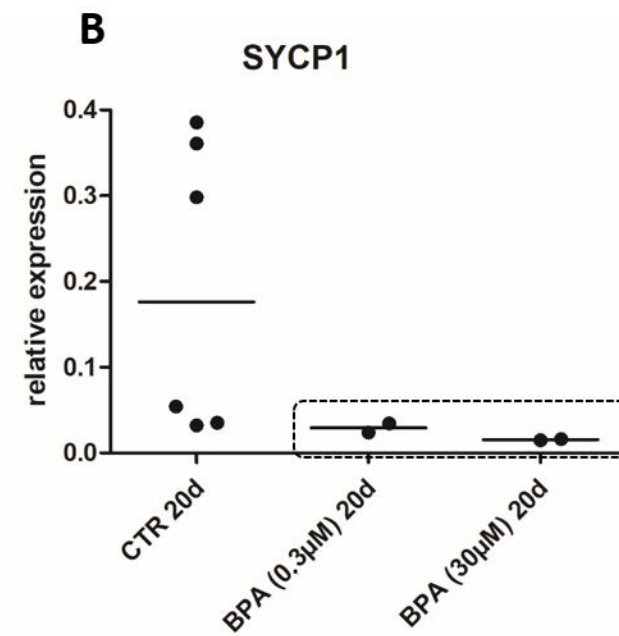
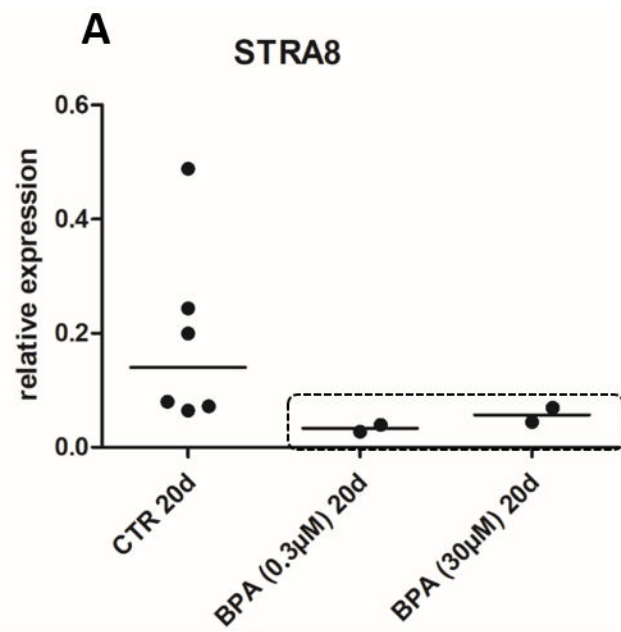


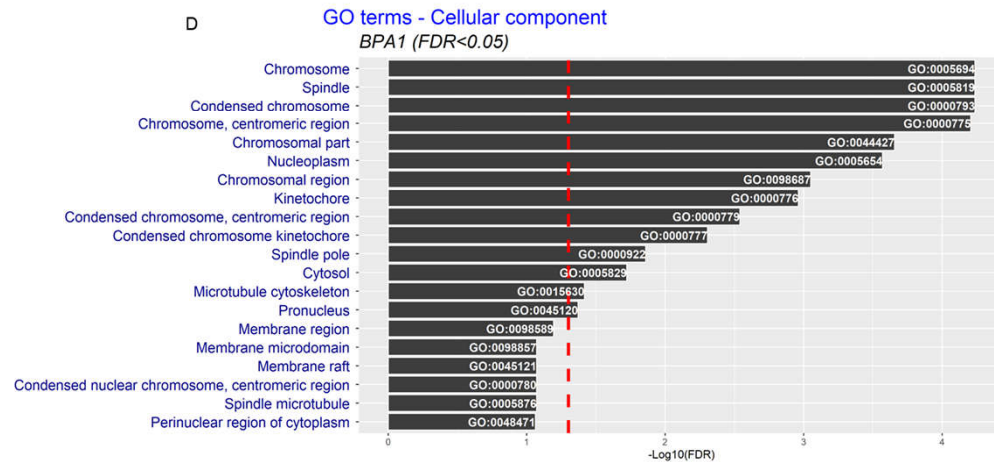
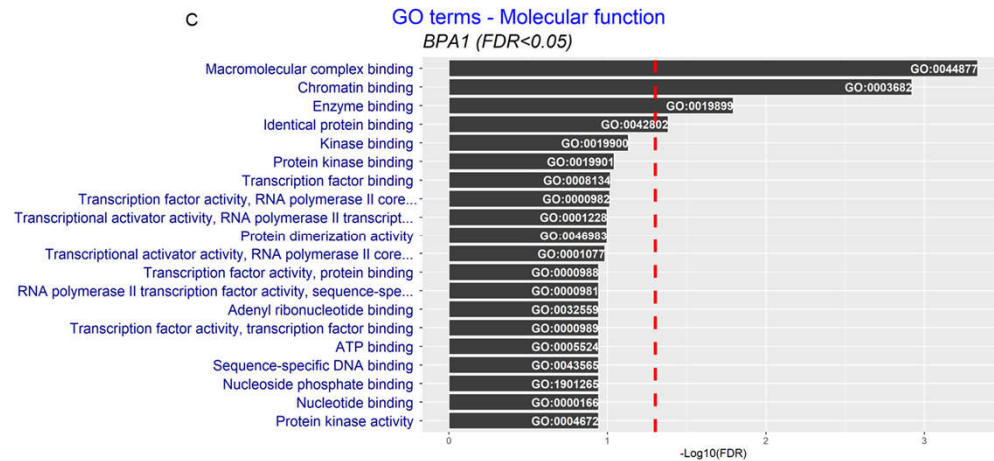
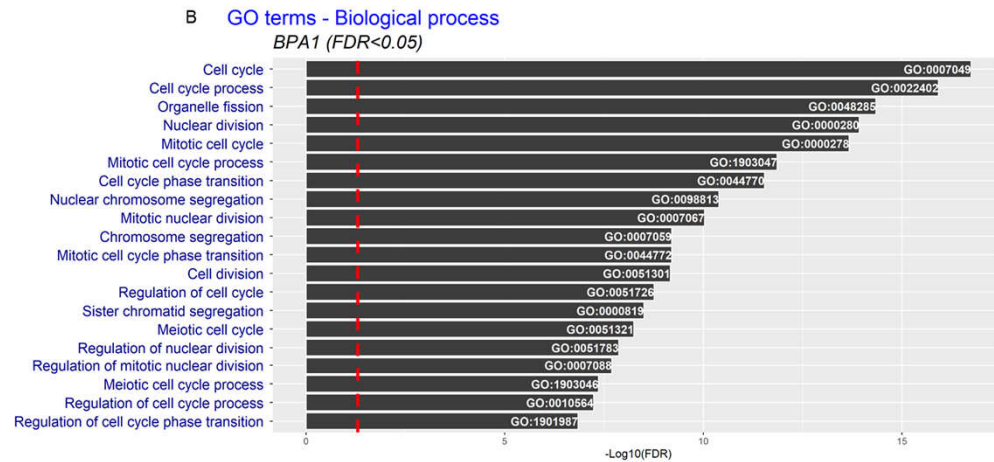
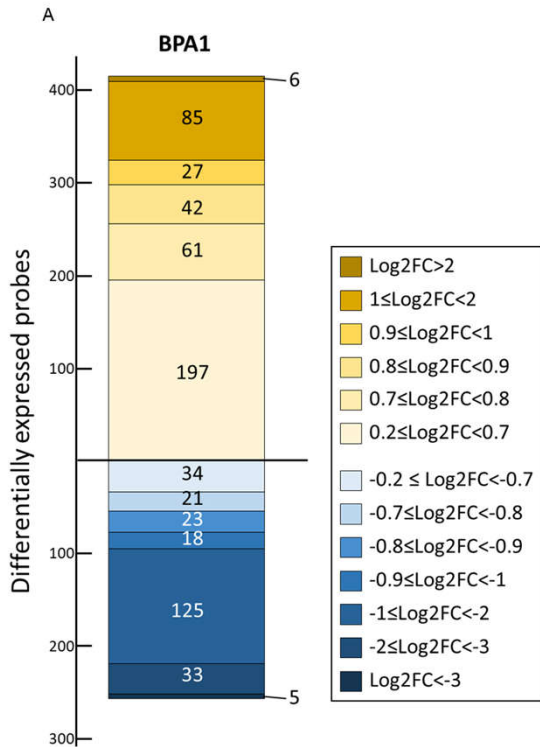
Figure 2

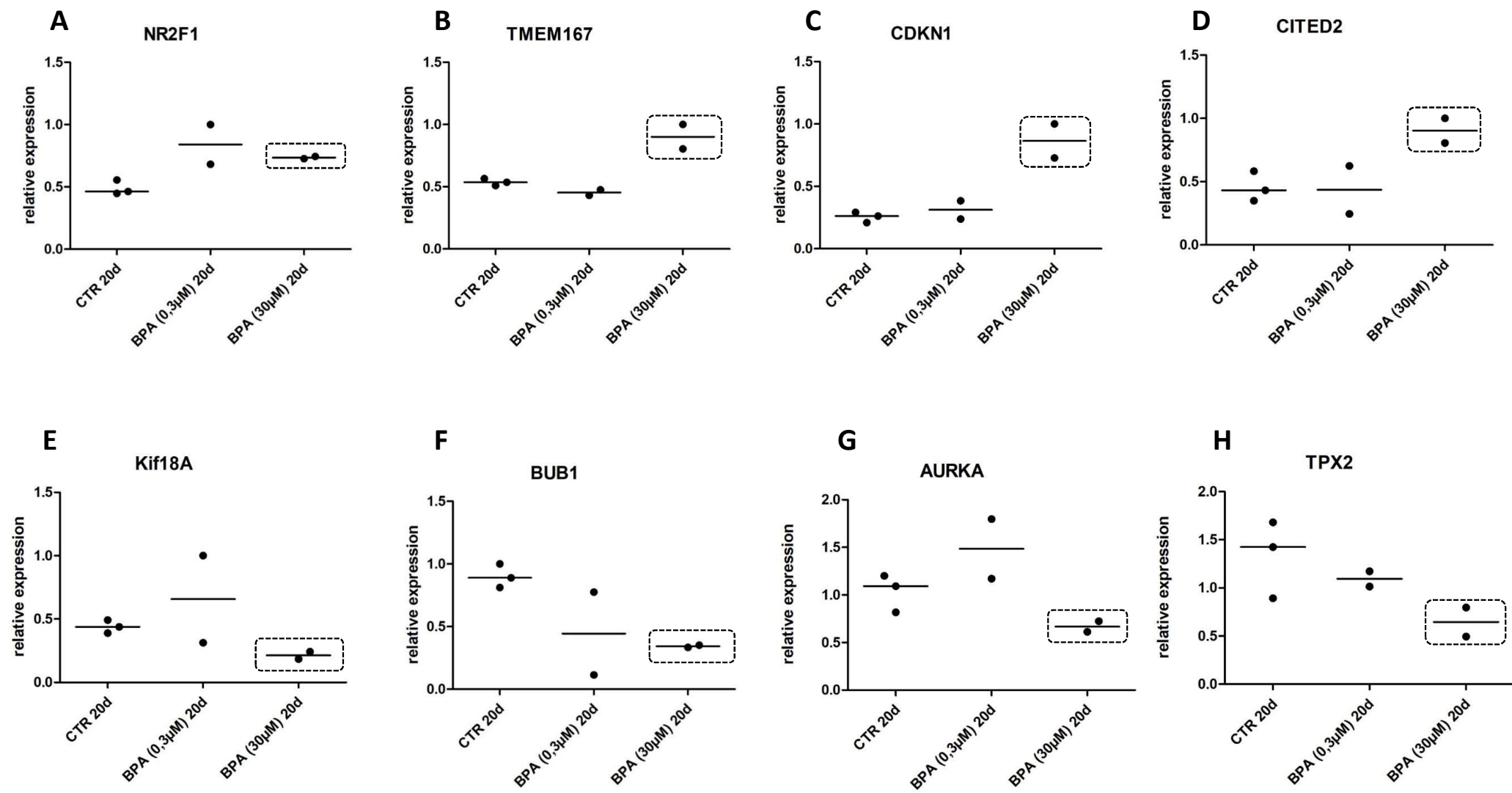
[Click here to access/download;Figure;Figure 2.pdf](#)













**Declaration of interests**

The authors declare that they have no known competing financial interests or personal relationships that could have appeared to influence the work reported in this paper.

The authors declare the following financial interests/personal relationships which may be considered as potential competing interests:

Benoit Loup  
Elodie Pומרol  
Luc Jouneau  
Paul A. Fowler  
Corinne Cotinot  
Béatrice Mandon-Pépin



Click here to access/download  
**Supplementary Material**  
Table S1\_final.xlsx





Click here to access/download  
**Supplementary Material**  
Table S2\_BMP.xlsx





Click here to access/download  
**Supplementary Material**  
Figures suppl S1.pdf

